Proteomic Stratification of Prognosis and Treatment Options for Small Cell Lung Cancer

Zitian Huo[1,2,3,#], Yaqi Duan[1,2,3,#], Dongdong Zhan[4,#], Xizhen Xu[5,#], Nairen Zheng[6,#], Jing Cai[7], Ruifang Sun[8], Jianping Wang[6,9], Fang Cheng[4], Zhan Gao[6], Caixia Xu[6], Wanlin Liu[6], Yuting Dong[1,2], Sailong Ma[1,2,3], Qian Zhang[1,2], Yiyun Zheng[1], Liping Lou[1], Dong Kuang[1], Qian Chu[5], Jun Qin[4,6], Guoping Wang[1,2,3,*], Yi Wang[6*]

[1.] *Institute of Pathology, Tongji Hospital, Huazhong University of Science and Technology, Wuhan 430030, China*

[2.] *Department of Pathology, Tongji Medical College, Huazhong University of Science and Technology, Wuhan 430030, China*

[3.] *National Health Commission Key Laboratory of Respiratory Diseases, Tongji Hosptial, Huazhong University of Science and Technology, Wuhan 430030, China*

[4.] *Beijing Pineal Diagnostics Co., Ltd. Beijing, 102206, China*

[5.] *Department of Oncology, Tongji Hospital, Tongji Medical College, Huazhong University of Science and Technology, Wuhan 430030, China*

[6.] *State Key Laboratory of Proteomics, Beijing Proteome Research Center, National Center for Protein Sciences (Beijing), Beijing Institute of Lifeomics, Beijing 102206, China*

[7.] *Institution of Pathology, The First Affiliated Hospital of Henan University, Kaifeng 450052, China*

[8.] *Department of Tumor Biobank, Shanxi Provincial Cancer Hospital, Taiyuan 030013, China*

[9.] *Chongqing Key Laboratory of Big Data for Bio Intelligence, School of Bioinformation, Chongqing University of Posts and Telecommunications, Chongqing 400065, China*

[#] Equal contribution.

*Corresponding authors.

E-mail: wangyi@ncpsb.org.cn (Wang Y); wanggp@hust.edu.cn (Wang G).

Running tile: *Huo Z et al / Proteomic stratification of SCLC*

Word count: 7539

References count: 69

Tables count: 0

Figures count: 5

Supplementary figures: 3

Supplementary tables:9

Title count:12

Running title count:4

Keywords count:5

Abstract count:196

Abstract

Small cell lung cancer (SCLC) is a highly malignant and heterogeneous cancer with limited therapeutic options and prognosis prediction models. Here, we analyzed formalin-fixed, paraffin-embedded (FFPE) samples of surgical resections by proteomic profiling, and stratified SCLC into three proteomic subtypes (S-I, S-II, and S-III) with distinct clinical outcomes and chemotherapy responses. The proteomic subtyping was an independent prognostic factor and performed better than current TNM or Veterans Administration Lung Study Group (VALG) staging methods. The subtyping results could be further validated using FFPE biopsy samples from an independent center, extending the analysis to both surgical and biopsy samples. The signatures of the S-II subtype in particular suggest potential benefits from immunotherapy. Differentially overexpressed proteins in S-III, the worst prognostic subtype, allowed us to nominate potential therapeutic targets, indicating that patient selection may bring new hope for previously failed clinical trials. Finally, analysis of an independent cohort of SCLC patients who had received immunotherapy validated the prediction that the S-II patients had better Progression Free Survival (PFS) and Overall Survival (OS) after first-line immunotherapy. Collectively, our study provides the rationale for future clinical investigations to validate the current findings for more accurate prognosis prediction and precise treatments.

Keywords: Small cell lung cancer; Proteomics; Prognosis; Chemotherapy response; Immunotherapy

Introduction

Small cell lung cancer (SCLC) is an exceptionally aggressive lung neuroendocrine neoplasm characterized by rapid tumor growth, early metastasis, and acquired chemo-resistance. Comprehensive whole-exome and whole-genome analyses have identified inactivation of *TP53* and *Rb1* as the predominant genetic alterations in SCLC, occurring in > 98% of the patients [1,2]. Genomic analysis of 51 SCLC cases also found genetic alterations in the PI3K/AKT/mTOR pathway in 36% of the samples, with mutations in *PIK3CA* (6%), *PTEN* (4%), *AKT2* (9%), *AKT3* (4%), *RICTOR* (9%), and *mTOR* (4%) [3]. However, effective stratification markers and treatment targets for SCLC remain limited [4]. As a result, the overall survival (OS) of SCLC patients has seen no significant improvement despite numerous clinical trials of different chemotherapy schemes and biological agents over the past decades [5]. Moreover, a lack of biomarkers that help predict efficacy has also impeded SCLC patients from reaping significant benefits from immunotherapy [6]. Currently, the 5-year survival rate is approximately 20-25% for limited-stage SCLC (LS-SCLC) and barely 1–2% for extensive-stage SCLC (ES-SCLC), making SCLC one of the deadliest cancers.

Early studies based on cell line morphologies classified SCLC into classic subtypes that expressed higher neuroendocrine (NE) markers and variant subtypes that showed low or an absence of neuroendocrine features [7,8,9,10]. These characteristics were further observed in clinical samples [11,12]. Subsequently, SCLC was classified according to the expression of neuroendocrine transcription factors ASCL1 and/or NEUROD1 [13]. Additionally, POU2F3 expression was used to define a non-NE, tuft-cell variant of SCLC [14]. And although YAP1 was proposed as a potential subtype marker for the remaining unclassified SCLC cases [3], it has yet to be confirmed [15]. Recently, re-analyzing previously published transcriptomic data classified SCLC into four subtypes [16]; in addition to the previously identified subtypes with the ASCL1 (SCLC-A), NeuroD1 (SCLC-N), and POU2F3 (SCLC-P) signatures, a new subtype (SCLC-I) characterized by the expression of inflammation gene signatures was uncovered.

In IMpower133, a global phase I/III, double-blind, randomized, placebo-controlled trial, atezolizumab (anti–PD-L1) was added to carboplatin + etoposide for ES-SCLC. SCLC-I patients were reported to experience the greatest benefit from this combined immuno- and chemotherapy. In the randomized, controlled, open-label, phase 3

CASPIAN trial, first-line durvalumab plus platinum-etoposide also significantly improved overall survival in patients with ES-SCLC versus a clinically relevant control group [17]. Additionally, cisplatin treatment of SCLC-A patient-derived xenografts induced intratumoral shifts toward SCLC-I [16]. These analyses suggest that the SCLC-I subtype might be the right candidate for immunotherapy. Therapeutic vulnerabilities were also identified for each subtype, including to inhibitors of PARP (SCLC-P), Aurora kinases (SCLC-N), or BCL-2 (SCLC-A) [16]. More recently, single-cell transcriptome sequencing (scRNA-seq) and imaging techniques have further revealed the heterogeneity and tumor microenvironment (TME) of SCLC [18]. Monocytes/macrophages appear to play a profibrotic and immunosuppressive role in SCLC TME. SCLC-N showed less immune infiltrate and greater T cell dysfunction than SCLC-A. More importantly, most SCLC cases share a small PLCG2-high subpopulation, which is linked to metastasis and poor prognosis.

While subtyping based on genomic and transcriptomic analyses has greatly improved our understanding of SCLC, the resulting subtypes correlated poorly with clinical outcomes. In contrast, subtyping with proteomics had revealed its exceptional clinical potential for more accurate predication of prognosis, chemo-sensitivity, and treatment targets for myriad cancers including stomach [19,20], liver [21,22], ovarian carcinoma [23] , colorectal cancer [24], and NSCLC [25,26,27,28,29]. Here, we report a proteomic subtyping model derived from a discovery dataset containing 75 surgically resected formalin-fixed, paraffin-embedded (FFPE) samples. The model was then validated in an independent cohort of 52 FFPE biopsy samples. The subtypes based on our proteomic model correlated well with clinical information including OS, and also allowed subtype-specific nomination of drug targets in SCLC. In addition, analysis of another 52 samples from patients who received immunotherapy allowed us to validate the finding that one particular proteimic subtype is an immune responsive subtype.

Results

Limited predictive power of SCLC staging and classification systems

In an effort to develop a more reliable SCLC subtyping system, we first analyzed the 75 surgically resected formalin-fixed, paraffin-embedded (FFPE) SCLC samples as shown in **Figure 1**A. Key clinical characteristics of the patients in the discovery cohort are presented in Figure 1B, with their detailed clinical and pathological data provided in

133 Table S1. Of the 75 cases, 62 (82.7%) were LS-SCLC and 13 (17.3%) were ES-SCLC
134 according to the Veterans Administration Lung Study Group (VALG) definition. Based
135 on the tumor-node-metastasis (TNM) staging system, 13 (17.3%), 19 (25.3%), 28
136 (37.3%) and 13 (17.3%) cases were categorized as stage I, II, III, IV, respectively. At the
137 end of follow-up, 31 (41.3%) patients survived, with a median overall survival (OS)
138 time of 2.78 ± 0.25 years. The statistically significant univariate prognostic factors
139 included age (Log-rank *P* value = 0.041), gender (Log-rank *P* value = 0.0085), and
140 lymph node metastasis (LNM (Log-rank *P* value = 0.041) (Figure S1).
141 When the predictive value of the current staging systems (including VALG and TNM)
142 were examined against actual prognosis of SCLC patients, their limitations became clear
143 (Figure 1C). In fact, only TNM I patients had significantly better OS than those of TNM
144 IV (Log-rank *P*-value = 0.04) (Figure 1C). Immunohistochemistry (IHC) was used to
145 examine the expression of ASCL1, NeuroD1, and YAP1 in the samples, and positive
146 rates of 81.3% (61/75), 20% (15/75), and 4% (3/75), were obtained respectively. Of all
147 cases, 11 were double-positive for ASCL1 and NeuroD1 (Figure S2 & Table S1).
148 However, classification based on ASCL1/NEUROD1 expression did not correlate with
149 OS differences in patients either (Figure 1C), although the NeuroD1^{+}/ASCL1^{-} subtype
150 showed better but not statistically significant prognosis (Log-rank test *P*=0.56).
151
152 **Proteomics stratifies SCLC into subtypes that correlate with clinical outcomes**
153 Since the current SCLC staging and classification systems failed to make a satisfactory
154 prediction, we carried out a proteomic study using these 75 samples by label-free
155 quantitative mass spectrometry (Figure 1A). We detected a total of 6,108 gene products
156 of high confidence from 75 samples, with 2957 proteins identified in more than 50%
157 samples. The protein identities and relative abundances of each case, designated as
158 fraction of total (FOT) [30], were provided in Table S2. To develop a robust
159 classification model, we first selected the top 1,100 most abundant proteins detected
160 from each sample, which yielded a dataset of 3,460 proteins; then the 445 proteins that
161 were detected in at least 7 samples (>10%) with the coefficient of variations (CV)
162 greater than 1.9 were used for non-negative matrix factorization (NMF) consensus
163 clustering (Table S3). NMF clustering yielded three subgroups, namely S-I (n=28, 37%),
164 S-II (n=20, 27%), and S-III (n=27, 36%) with the maximum average silhouette of 0.83
165 (**Figure 2**A). Importantly, these proteomic subtypes correlated well with overall survival
166 prognosis. Patients in S-I had the best overall survival with a 5-year OS probability of

167 75%, whereas S-III had the worst survival with only 3.7% of 5-year OS (Log-rank *P*-
168 value < 0.001) (Figure 2B). A multivariate Cox analysis confirmed that the proteomic
169 subtype was an independent prognostic factor (S-I vs S-III, HR = 4.73, 95% CI, 1.81-
170 12.4, Cox *P*-value = 0.002) after adjusting for TNM stage, VALG stage, and other
171 covariates including chemotherapy, age, gender, LN metastasis status, and smoking
172 history (Figure S3). These data indicated that proteomics-based subtyping is superior in
173 overall survival prognosis.
174
175 **The proteomic subtypes show different benefit of chemotherapy on prognosis**
176 The platinum agent (cisplatin or carboplatin) and etoposide-based combination
177 chemotherapy is the standard care for SCLC patients after surgery, although the
178 percentage of patients who actually benefit from such care is quite small [31]. In our
179 dataset, approximately half of the patients (33, 44%) underwent chemotherapy.
180 Considering the impact of TNM I and IV on prognosis mentioned earlier, we included
181 only TNM II and III patients for chemosensitivity analysis. As shown in Figure 2C,
182 chemotherapy exhibited different impact on prognosis for the three proteomic subtypes.
183 The S-I subtype benefited most significantly from chemotherapy (Log-rank *P*-value =
184 0.023), with all patients who received chemotherapy were still alive by the end of the
185 study. The S-II subtype appeared to have worse prognosis (Log-rank *P*-value = 0.042).
186 The S-III subtype had the worst prognosis and were chemo-insensitive (Log-rank *P*-
187 value = 0.15). In summary, our proteomic SCLC subtyping could stratify patients into 3
188 distinct subtypes that are more clinically relevant. The S-I subtype was chemo-sensitive
189 with the best OS. S-II had medium OS where chemotherapy might be detrimental. S-III
190 had the poorest prognosis and was insensitive to chemotherapy, suggesting that S-III
191 patients have the greatest need for new therapies.
192 To facilitate the validation of the subtyping in the independent external dataset, we
193 developed a random forest (RF) classifier with the discovery set. The top 500 most
194 abundant proteins detected in each sample were aggregated for differential expression
195 analysis. The resulted 58 signature proteins (Fold change > 1.5, adjusted t-test P-value <
196 0.05) with high identification frequencies (detected in more than 25% of the samples)
197 were used as input (predictor variables) (Table S4). We trained a random forest (RF)
198 classifier with a 10-fold cross-validation in the discovery dataset. Based on the 58
199 features, the predictive classifier model yielded a 90.8% accuracy for the discovery
200 dataset. We collected 52 SCLC biopsy samples from another center (the First Affiliated

201 Hospital of Henan University) as an independent validation dataset. The corresponding
202 clinical information of these samples is summarized in Table S5. This subset included 12
203 female and 40 male patients, with an overall survival time ranging from 0.019 to 4.493
204 years. The two-year survival rate was 8/52, or 15.4% and the three-year survival rate
205 was 2/52, or 3.8%. Proteomic analysis were performed on the 52 biopsy samples. The
206 results were listed in Table S6. When the RF classifier was applied to the validation
207 dataset, the predicted S-I, S-II, and S-III subtypes contained 8, 34, and 10 cases,
208 respectively. The prognosis trend was consistent with that of the discovery cohort, with
209 one-year survival rates of 87.5%, 52.9%, and 30.0% and two-year survival rates of
210 37.5%, 14.7%, and 0% for S-I, S-II, and S-III, respectively. Kaplan-Meier analysis
211 illustrated that the overall survival varied significantly among the three subtypes (Log-
212 rank test P = 0.007) (Figure 2D). Thus, the proteomic subtyping model derived from
213 surgical samples could be validated with biopsy samples from an independent center.
214

215 **Differential signature proteins and enriched biological processes in proteomic**
216 **SCLC subtypes**

217 To investigate the proteomic features of SCLC subtypes, we selected significantly
218 altered proteins by comparing their expression in each subtype to the other subtypes
219 (Wilcox test $P < 0.05$ and fold change > 3 for S-I and II or fold change > 10 for S-III).
220 As a result, 206, 162, and 126 subtype-specific proteins for S-I, S-II, and S-III
221 respectively were designated as significantly altered proteins. (**Figure 3**A, Table S7).
222 Functional enrichment using Metascape showed that the most distinct subtype was S-II,
223 which was significantly enriched in extracellular matrix, interferon gamma signaling and
224 neutrophil degranulation (adjusted P values were between 10^{-8}-10^{-17}) (Figure 3B). In the
225 regulation of immune functions, Major histocompatibility complex class I (MHC-I)
226 molecules play an important role in cell-mediated immunity by presenting tumor
227 antigens to CD8+ T cells and enabling cytotoxic T cells to recognize and eliminate
228 tumor cells. Antigen presenting cells (APCs) such as B cells, dendritic cells (DCs), and
229 monocytes/macrophages express major histocompatibility complex class II molecules
230 (MHC II) and present antigenic peptides to CD4+ helper T cells. Here, we found that the
231 MHC-I (including HLA-A, HLA-B, and HLA-C) but not the MHC-II (including HLA-
232 DQA1, HLA-DQB1, HLA-DRA, HLA-DRB1, HLA-DRB5, HLA-F and HLA-E)
233 molecules were expressed at higher levels in S-II than in the other two subtypes (Figure
234 3C & D). Moreover, TAP1, TAP2, and TAPBP were also highly overexpressed in S-II.

235 TAP1 and TAP2 are members of the superfamily of ATP-binding cassette (ABC)
236 transporters that shuttle various molecules across extra- and intra-cellular membranes.
237 The ATP-loaded TAP1-TAP2 complex mediates unidirectional translocation of peptide
238 antigens from the cytosol to endoplasmic reticulum (ER) for their loading onto MHC
239 class I (MHC-I) molecules [32]. TAPBP is a transmembrane glycoprotein that mediates
240 interactions between newly assembled MHC-I molecules and TAP proteins, and is
241 required for the transport of antigenic peptides across ER membrane[33]. Thus, the S-II
242 subtype is characterized by an enrichment of factors involved in antigen presentation.
243 The S-I subtype appeared to be marginally enriched in proteins functioning in
244 transport, membrane trafficking, and RNA metabolic processes (adjusted *P* values of 10^{-}
245 ^{2}-10^{-4}). Detailed analysis identified ubiquitin-mediated proteolysis in cell cycle control,
246 including the anaphase promoting complex (ANAPC1, ANAPC13, and ANAPC4) and
247 COPS9 signalosome components (COPS3 and COPS7B) as well as NEDD8. DNA
248 repair and DNA replication proteins, including MSH3, LIG1, POLE3, RFC3, ORC2,
249 and ATM, were also enriched (Table S7). After adjusting for *P* values, Metascape
250 analysis could not identify significantly enriched biological processes for S-III. Manual
251 inspection showed that proteins in chromatin organization/transcription regulation as
252 well as various enzymes were enriched (Table S7). Among them were proteins
253 mediating chromatin assembly and telomere maintenance (CHAF1A, TERF2, and
254 TOX4), transcription coactivators (e.g., ATAD2, ZNF516, PHF6, PHF8, MED6, TAF5,
255 and TAF) and corepressors (e.g., TBL1X, TBL1Y, CHD8, ATXN2, and SPEN). It
256 appears that mis-regulation in chromatin structure and transcription may profoundly
257 impact an array of biological processes, which the Metascape algorithm might have
258 failed to identify.
259
260 **The S-II patients had the best immunotherapy responses in SCLC**
261 Our analysis above suggested that S-II was an inflamed SCLC subtype in nature, which
262 may benefit from immunotherapy. To test this hypothesis, we collected another 52 real-
263 world FFPE biopsy or surgery samples from ES-SCLC patients who received Immune
264 checkpoint inhibitors (ICIs) (including Sintilimab, Toripalimab, Durvalumab,
265 Camrelizumab, Tislelizumab, and Atezolizumab). Among them, 37 were treated with
266 combined immunotherapy with chemotherapy as a first-line treatment, and 49 were from
267 biopsy (**Figure 4**A & Table S8). We classified these samples using the model derived
268 from the discovery dataset (Table S9) into S-I (23 patients), S-II (13 patients), and S-III

(16 patients). We specified an Immune checkpoint inhibitors PFS (ICI-PFS) as the duration between the time when the first immunotherapy was applied, and Progressive Disease (PD) was determined by clinical standards. As shown in Figure 4B&C, the ICI-PFS of the S-II patients with first-line ICIs rather than > first line ICIs was significantly longer than those of S-III (Log-rank test $P = 0.04$), and S-I (Log-rank test $P = 0.08$). Moreover, when the K-M plots of the S-II patients in the immunotherapy cohort, the discovery cohort (WH-S-II, no immunotherapy) (Log-rank test $P = 0.03$) and the validation cohort (HN-S-II, no immunotheray) (Log-rank test $P < 0.0001$) (Figure 4D) were compared, the S-II patients achieved better OS when trated with immunotherapy. Together, these analyses demonstrated the values of stratifying patients for immunotherapy, and suggested that immunotherapy could significantly improve the OS of SCLC patients, particularly for those in the S-II subtype.

Potential drug repurposing targets for S-III subtype patients

Since patients in the S-III subtype had the worst OS and did not benefit from chemotherapy, they were the most in need of new therapeutic options. We selected specifically overexpressed proteins in S-III compared with S-I and S-II and investigated their feasibility as potential drug repurposing targets. We first identified previously investigated actionable drug targets and found that at least one target among EGFR, AURKB, BCL2, and EZH2 was highly expressed in a total of 21/27, or 77.8% of S-III patients. Drugs targeting AURKB, BCL2, or EZH2 are currently in various stages of clinical development and have shown promising results for treating certain cancers [34,35,36]. Many kinases, phosphatases, transporters, UPS proteins, and other enzymes were overexpressed in S-III, accounting for nearly 1/3 of all specifically overexpressed proteins in S-III. Proteins that regulate necroptosis, including MLKL, TRAF2, and RIPK1 are also potential targets [37]. Their druggability needs to be further investigated. An overview of the potential drug repurposing targets for each individual patient is shown in **Figure 5**.

Discussion

While genomic and transcriptomic analyses have greatly improved our understanding of SCLC tumorigenesis, their values in identifying effective stratification markers and therapeutic targets are limited. In this retrospective proteomic analysis, we showed that proteomics alone could stratify SCLC for prognosis and chemo-sensitivity. Since most

303 SCLC tumors are non-resectable when diagnosed, we validated our proteomic subtyping
304 using biopsy samples from an independent center, expanding the clinical utility of our
305 proteomic subtyping method. Our analysis shows that all S-I patients in the discovery
306 cohort who received chemotherapy were alive by the end of the study, confirming the
307 suitability of chemotherapy as first line treatment option for these patients. Antigen
308 presentation and other immune responses were enriched in S-II, suggesting that immune
309 checkpoint inhibitors (ICIs) may be a viable choice for S-II patients. We validated this
310 prediction in a third independent group of patients that received immunotherapy as the
311 first-line treatment. Notably, a previous transcriptomic study also defined an "inflamed"
312 SCLC subtype (SCLC-I) [15] characterized by high expression of genes related to HLAs
313 and experienced greatest benefit from the addition of anti-PDL1 to chemotherapy [15].
314 Our proteomic subtyping thus may provide value in guiding SCLC treatment.

315 Since neither PDL1 expression nor TMB is a reliable biomarker for the prediction of
316 immunotherapy response in clinical trials such as IMPower133 and CheckMate032,
317 other biomarkers are in great need. Our analysis showed that patients in the S-II subtype
318 may benefit from the immunotherapy. Although they were mostly ES-SCLC and lost the
319 oppotunity for surgery, the two-year survival rate of the S-II patients with
320 immunotherapy reached over 30%, much better than the other subtypes. In other clinical
321 trials (for example, ASTRUM-005), the median PFS was generally less than 6 months
322 [38], which was similar to that of S-I/III patients in our study. However, the median PFS
323 reached around one year for the S-II subtypes here. It will be important to investigate in
324 a prospective trial to determine whether the S-II subtype could serve as a new predictive
325 biomarker for guiding SCLC immunotherapy.

326 Mechanisms of immune resistance vary [39]. MHC-I molecules were generally
327 expressed at low levels in the SCLC tumor cells, resulting in low antigen presentation.
328 In addition, tumor cells can also secrete factors to inhibit antigen presenting cells. About
329 50% of patients with SCLC have almost no T cell infiltration, and there are also
330 suppressive immune cells in the immune microenvironment of SCLC. In our study, S-II
331 subtype had both higher MHC-I molecules, along with other proteins in antigen
332 presenting. Interferon gamma signaling was also enriched in S-II. Thus, S-II may be the
333 immune hot subtype while S-I/III were the cold ones.

334 Among proteins and pathways as potential drug targets for the S-III subtype, BCL2,
335 EZH2, ARUKB, and EGFR are actionable drug targets that have been at various stages
336 of clinical trials. Among them, EZH2 was identified as an upstream regulator in the

337 SLFN11 axis that mediates acquired chemoresistance in an *in vitro* PDX model [40].
338 FDA has recently approved the EZH2 inhibitor tazemetostat for treating epithelioid
339 sarcoma [41]. Interestingly, EZH2 is a negative regulator of MHC class I molecules, and
340 inhibiting EZH2 could enhance antigen presentation and circumvent anti-PD-1
341 resistance [42].

342 Although EGFR-TKi (such as Gefitinib) was not effective in a SCLC clinical trial
343 [43], the identification of a subgroup of patients with EGFR overexpression suggest an
344 alternative approach by using EGFR antibody. Notably, EGFR antibody has been
345 approved as first-line treatment option for KRAS wildtype, EGFR overexpressing colon
346 cancer patients [44]. BCL2 family proteins comprise the sentinel network that regulates
347 mitochondrial and intrinsic apoptotic responses. Previous studies of a BCL-2 inhibitor
348 fell short of expectations in SCLC clinical trials [45]. A possible explanation is that
349 patients in the trial were not screened for BCL-2 expression. Interestingly, the SCLC-A
350 transcriptomic subtype [15], which had higher expression of BCL2, was found to be
351 sensitive to multiple BCL2 inhibitors in an *in vitro* study. Recently, the single target
352 BCL2 inhibitor Venetoclax, which was approved by the FDA for acute myeloid
353 leukemia and chronic lymphocytic leukemia [46], showed therapeutic effect on multiple
354 patient-derived xenografts of SCLC [47]. AURKB is a mitotic protein kinase. Phase I/II
355 clinical studies of its inhibitor Alisertib have demonstrated increased antitumor effects in
356 various hematologic malignancies and solid tumors [48].

357 In addition, our proteomic data suggested that necroptosis regulators including
358 MLKL, TRAF2, and RIPK1 may be investigated as potential therapeutic targets for
359 SCLC. Necroptosis causes cellular swelling and plasma membrane collapse, which may
360 lead to the release of intracellular biomolecules including damage-associated molecular
361 patterns (DAMPs) and cytokines. These molecules can perform immunological
362 functions such as chemotaxis, phagocytosis, and immune cell activation [49]. Although
363 initial attraction of antigen presentation cells such as macrophages and dendritic cells
364 (DCs) by DAMPs/cytokines could recruit CD8/CD4 positive T cells for immune
365 activation in early stage, the recruitment of myeloid-derived suppressor cells (MDSC)
366 and tumor-associated macrophages (TAM) at later stages could lead to immune
367 suppression [50]. The effects of necroptosis proteins on tumors are cancer dependent.
368 Cytokines released by necroptotic cancer cells can promote tumor angiogenesis,
369 proliferation, and metastasis. For instance, high expression of RIPK1 was linked to
370 metastasis in breast cancer [51] and poor survival in glioblastoma [52] but was a good

371 prognostic indicator in head and neck cancer [53]. High MLKL expression correlated
372 positively with good prognosis in colorectal cancer [54], HR-HPV cervical cancer (high
373 risk-human papillomavirus) [55], ovarian cancer [56], and pancreatic adenocarcinoma
374 [57], but negatively in breast cancer [58], cervical squamous cell carcinoma [59], and
375 gastric cancer [60]. We found in this study a correlation between high expression of
376 MLKL, TRAF2, and RIPK1 and the most malignant SCLC S-III subtype, suggesting
377 that these proteins may represent good targets for treating SCLC.

378 The S-III subtype is also enriched in proteins involved in chromatin organization and
379 transcriptional regulation. For example, CHAF1A, TERF2, and TOX4 can mediate
380 chromatin assembly, protect chromosome ends, and regulate chromatin binding during
381 DNA replication [61], metaphase [62], and transition to interphase [63], respectively.
382 For transcriptional regulation, ATAD2 and ZNF516 act as transcription activators,
383 promoting the expression of CCND1/MYC/ E2F1 [64] or genes related to cellular
384 response to replication stress [65], respectively. Moreover, PHF8 acts as a coactivator of
385 rDNA transcription by activating polymerase I (pol I) mediated transcription of rRNA
386 genes [66] , while MED6 is a coactivator involved in the regulated transcription of
387 nearly all RNA polymerase II-dependent genes [67]. These findings underline the
388 importance of investigating dysfunctional chromatin organization in the development
389 and treatment of SCLC.

390 Our study has some limitations. For example, our discovery cohort was relatively
391 small compared with other omics studies, such as those of NSCLC. This is in part
392 because most SCLC cases were detected at late stages without opportunity for surgery,
393 so large-scale proteomic analysis of surgically resected samples was rare in the past.
394 Moreover, our proteomic stratification was different from previous transcriptional
395 classification based on ASCL1, NeuroD1, and YAP1, thus providing limited mechanistic
396 insight into the tumorigenesis. The reason for the discrepancy is unclear, but we did
397 notice by IHC the overlap of several of these markers.

398 In summary, our results demonstrate the validity and importance of using both
399 surgical and biopsy FFPE samples and serve as a valuable resource for the SCLC
400 research community. This work should also help guide future pre-clinical investigations
401 that seek more meaningful and efficacious stratification of SCLC in order to improve
402 therapeutic responses and patient survival.
403

404 ## Materials and methods

405 **Sample collection**

406 Tumors in the discovery cohort (diagnosed from 2012 to 2018) were obtained with
407 informed consent from archival sources at Tongji Hospital, Tongji Medical College,
408 Huazhong University of Science and Technology. Tumors in the second cohort
409 (diagnosed from 2018 to 2021) were biopsy samples obtained from the First Affiliated
410 Hospital of Henan University. The 52 samples in the immunotherapy cohort was also
411 from Tongji Hospital (diagnosed from 2017 to 2021). The samples were collected from
412 patients at initial diagnosis. All diagnoses were independently reviewed by three
413 experienced pathologists, and complied with the latest World Health Organization
414 classification standards. The tumors came from patients not treated with neoadjuvant
415 chemotherapy or radiotherapy before operation, with no previous history of malignancy,
416 having SCLC as the initial primary cancer diagnosis at the time of surgical resection,
417 and with adequate tumor/tissue material as well as clinical annotation and follow-up
418 time. The tumor cell content were >90% tumor cells judged by haematoxylin and eosin
419 (H&E) staining and yielded >700 proteins in MS analysis. All cases were staged
420 according to the National Comprehensive Cancer Network (NCCN) clinical practice
421 guidelines in oncology for small cell lung cancer (version 4.2020).

422

423 **Immunohistochemistry and assesment**

424 Immunohistochemical staining was conducted using tissue arrays. Prior to de-
425 paraffinization, the slides were heated to 60°C for ten minutes to melt the paraffin. The
426 slides were then washed three times with xylene to solubilize and remove the paraffin.
427 Next, the xylene was removed by washing three times with 100% ethanol followed by
428 75%, 50% ethanol, and PBS. After the sections were deparaffinized and hydrated, the
429 endogenous peroxidase activity was blocked. Antigen retrieval was performed using the
430 Dako Target Retrieval Solution, High pH (Dako Ominis, Agilent Technologies, CA,
431 USA), in a PTLink set at 98ºC for 25 min. The slides were then incubated with the
432 primary antibody at 4 ℃ overnight.

433 Primary antibodies used in this study were: anti-ASCL1 antibody (Abcam, ab211327,
434 1:200, Boston, MA), anti-NeuroD1 antibody (Abcam, ab213725, 1:200,), and anti-YAP1
435 antibody (Abcam, ab52771, 1:50,). Following secondary antibody incubation (~1 hour),
436 the sections were visualized with the DAB kit (ZLI-9017, Zhongshan Biotechnology,

437 China) and counterstained with hematoxylin. The stained samples were scored by three
438 pathologists independently for the multiplication of staining intensity (1- weak; 2-
439 moderate; 3- strong) and the percentage of positive tumor cells, which resulted in scores
440 of 0-300. A score of < 10 was designated as 0, 10-40 as 1+, 41-140 as 2+, and 141-300
441 as 3+. All samples with scores of > 10 were considered positive cases.
442
443 **Protein extraction, trypsin digestion, and LC-MS/MS processing**
444 For each SCLC sample, proteins were extracted from three tissue slices (5-µm thick)
445 from the FFPE block (2-5 mm in diameter) The de-paraffinization procedure was the
446 same as IHC as described above. Air dried sample was scraped from the slide and
447 resolubilized in 100 ml of 50 mM NH_4HCO_3. The sample was then incubated at 95°C
448 for 5 min for de-crosslinking, and cooled to room temperature. Trypsin digestion was
449 carried out at 37°C overnight. Peptides were extracted twice with 200 µl of extraction
450 buffer (50% acetonitrile and 0.1% formic acid in water) with 15 min vortex. The
451 resulting peptides were dried and stored at -80°C for future analysis. The digested
452 peptides were eluted, divided into three fractions, and analyzed on a Q Exactive HF-X or
453 Orbitrap Exploris™ 480 mass spectrometer coupled with an Ultimate 3000 RSLCnano
454 LC system (Thermo Fisher Scientific) and operated at data-dependent aquisition mode.
455 MS1 was measured in the Orbitrap at a resolution of 60,000 followed by tandem MS
456 scans of the top 40 precursors using higher-energy collision dissociation with 27% of
457 normalized collision energy and 15 s of dynamic exclusion time.
458
459 **Mass spectrometry data analysis**
460 MS Raw files were searched against the National Center for Biotechnology Information
461 (NCBI) Ref-seq human proteome database (updated on 04/07/2013, 27,414 entries) in
462 Firmiana [68], a one-stop proteomic cloud platform for data processing and analysis,
463 implemented with Mascot search engine with Percolator (Matrix Science, version
464 2.3.01). The following search parameters were used: (1) Mass tolerances were 20 ppm
465 for precursor ions and 0.05 Da for product-ions; (2) Up to two missed cleavages were
466 allowed; (3) The minimal peptide length was seven amino acids; (4) Cysteine
467 carbamidomethylation was set as a fixed modification, and N-acetylation and
468 methionine oxidation were considered variable modifications; and (5) The charges of
469 precursor ions were limited to +2, +3, +4, +5, and +6. The peptide and protein FDR

470 were both set to 1%. A label-free, intensity-based absolute quantification (iBAQ)
471 algorithm was used for protein quantification. The iBAQ values were calculated by
472 dividing the raw intensities by the number of theoretical observable peptides. FOT
473 (fraction of total), calculated by dividing a protein's iBAQ by the sum of iBAQs of all
474 identified proteins in a single experiment, was used as normalized abundance to
475 compare protein abundance across all experiments. The missing value was imputed with
476 1/10 of the global non-zero minimum value of the sample [69].
477
478 **Subtyping and validation**
479 A non-negative matrix factorization (NMF) consensus clustering algorithm was used for
480 subtyping the discovery dataset. The standard "brunet" option was selected and 50
481 iterations were performed. The number of clusters (k) was set as 2 to 6, and the
482 minimum member of each subclass was set as 10. The silhouette indicator (Average
483 silhouette > 0.8) and prognostic association (*P*-value < 0.01) were used to determine the
484 optimal clustering number.
485 To develop a robust classification model, we first selected the top 1,100 most
486 abundant proteins detected from each sample, which yielded a dataset of 3,460 proteins;
487 then the 445 proteins that were detected in at least 7 samples (>10%) with the coefficient
488 of variations (CV) greater than 1.9 were used for non-negative matrix factorization
489 (NMF) consensus clustering (Table S3)
490 To validate the classification in an independent external dataset, the random forest
491 (RF) classifier was implemented on the discovery set using the R function randomForest
492 (package: randomForest). The top 500 most abundant proteins detected in each sample
493 were aggregated for differential expression analysis. Finally, 58 significantly
494 differentially expressed proteins (Fold change > 1.5, adjusted t-test *P*-value < 0.05) with
495 high identification frequencies (detected in more than 25% of the samples) were used as
496 input (predictor variables). The subtype terms of SCLC on the discovery set were used
497 as the response variables. The optimal parameters were estimated from the R function
498 train (package: caret). The 10-fold cross-validation strategy was utilized for internal
499 validation.
500
501 **Survival analysis**
502 The Kaplan-Meier method, log-rank test, and the Cox proportional-hazards model with
503 Wald statistics were used for survival analysis in all datasets. The multivariate Cox

analysis was adjusted for age, sex, staging system, and chemotherapy. Hazard ratios (HRs) with 95% confidence intervals (CI) were estimated for each variable. All calculated *P*-values were two-sided where <0.05 was considered statistically significant.

Bioinformatic analysis

To investigate the proteomic features of SCLC subtypes, we selected significantly altered proteins by comparing their expression in each subtype to the other subtypes (Wilcox test $P < 0.05$ and fold change > 3 for S-I and II or fold change > 10 for S-III). Metascape analysis was conducted online (https://metascape.org) for functional pathway analysis. The on-line tool (Sangerbox tools, http://www.sangerbox.com/tool) was used for generating the plots and heatmap. All other statistical analyses were carried out with R 3.6.1.

Ethical statement

This study was approved by the ethical committee of Tongji Hospital, Tongji Medical College, Huazhong University of Science and Technology (Approval Number: TJ-IRB20201011).

Data availability

All data and search results have been deposited to the iProX database (http://www.iprox.org) with the iProX accession: IPX0004230000.

Acknowledgments

This work was supported by the National Key R&D Program of China (Grant Nos. 2018YFA0507503, 2017YFA0505102, 2017YFA0505103, and 2017YFA0505104), the National Natural Science Foundation of China (Grant Nos. 82072597, 62131009, 31770892, 31970725, 31870828, 81874237, and 81974016), Beijing Municipal Natural Science Foundation (Grant No. 7192199), and State Key Laboratory of Proteomics (Grant No. SKLP-K202002), Kaifeng science and technology development plan project (Grant No. 1806005). We thank the Mass Spectrometry Platform of National Center for Protein Sciences (Beijing) (Phoenix Center) for technical assistance. We also thank all the patients who participated in this study, as well as the clinicians and staff of the institutions who assisted with the studies.

CRediT author statement

Zitian Huo: Writing - original draft,Formal analysis, Investigation,Visualization

Yaqi Duan:Writing - review & editing.Methodology.

Dongdong Zhan: Investigation, Data curation,Validation

Xizhen Xu: Visualization,Writing - review & editing.

Nairen Zheng: Data curation. Validation.

Jing Cai: Data curation. Resources.

Ruifang Sun: Resources, Data curation.

Jianping Wang: Resources, Data curation.

Fang Cheng: Resources, Data curation.

Zhan Gao: Resources, Data curation.

Caixia Xu: Resources, Data curation.

Wanlin Liu: Resources, Data curation.

Yuting Dong: Resources, Data curation.

Sailong Ma: Resources

Qian Zhang: Resources

Yiyun Zheng: Resources

Liping Lou: Resources

Dong Kuang: Writing - review & editing.

Qian Chu: Supervision, Project administration, Funding acquisition.

Jun Qin: Conceptualization, Resources, Supervision, Project administration, Funding acquisition.Writing - review & editing.

Guoping Wang: Conceptualization, Resources, Supervision, Project administration, Funding acquisition.

Yi Wang: Conceptualization, Resources, Supervision, Project administration, Funding acquisition.Writing - review & editing.

All authors read and approved the final manuscript.

Conflict of interest

Jun Qin and Yi Wang are cofounders and co-owners of the Beijing Pineal Diagnostics Co. Ltd.; Dongdong Zhan and Fang Cheng are employees of the Beijing Pineal Diagnostics Co. Ltd.. All the other authors declare no competing interests.

ORCID

0000-0002-7368-0831(Zitian Huo)
0000-0002-2392-5642 (Yaqi Duan)
0000-0002-0704-8782 (Dongdong Zhan)
0009-0000-3222-6862(Xizhen Xu)
0000-0002-3952-1570 (Nairen Zheng)
0000-0001-8002-2645(Jing Cai)
000-0002-4791-3734 (Ruifang Sun)
0000-0001-6142-7153 (Jianping Wang)
0000-0001-9385-204X (Fang Cheng)
0009-0001-9697-6547 (Zhan Gao)
0009-0003-1014-1448 (Caixia Xu)
0000-0002-4116-2597 (Wanlin Liu)
0000-0003-0886-9221 (Yuting Dong)
0009-0007-5118-6991 (Sailong Ma)
000-0002-0869-3951 (Qian Zhang)
0000-0001-8103-3688 (Yiyun Zheng)
0000-0002-9542-568X (Liping Lou)
000-0001-9558-0333 (Dong Kuang)
0000-0001-8192-7630 (Qian Chu)
0000-0003-3769-3720 (Jun Qin)
0009-0000-6472-0849 (Guoping Wang)
0000-0002-2088-2085 (Yi Wang)

References

[1] Rudin CM, Durinck S, Stawiski EW, Poirier JT, Modrusan Z, Shames DS, et al. Comprehensive genomic analysis identifies SOX2 as a frequently amplified gene in small-cell lung cancer. Nat Genet 2012;44:1111–6.

[2] George J, Lim JS, Jang SJ, Cun Y, Ozretić L, Kong G, et al. Comprehensive genomic profiles of small cell lung cancer. Nature. 2015;524(7563):47-53. doi:10.1038/nature14664

[3] Umemura S, Mimaki S, Makinoshima H, Tada S, Ishii G, Ohmatsu H, et al. Therapeutic priority of the PI3K/AKT/mTOR pathway in small cell lung cancers as revealed by a comprehensive genomic analysis. J Thorac Oncol. 2014;9(9):1324-1331. doi:10.1097/JTO.0000000000000250

[4] Rudin CM, Poirier JT, Byers LA, Dive C, Dowlati A, George J,et al. Molecular subtypes of small cell lung cancer: a synthesis of human and mouse model data [published correction appears in Nat Rev Cancer. 2019 Jun 7;:]. Nat Rev Cancer. 2019;19(5):289-297. doi:10.1038/s41568-019-0133-9

[5] Gazdar AF, Bunn PA, Minna JD. Small-cell lung cancer: what we know, what we need to know and the path forward [published correction appears in Nat Rev Cancer. 2017 Nov 10;:]. Nat Rev Cancer. 2017;17(12):725-737. doi:10.1038/nrc.2017.87

[6] Iams WT, Porter J, Horn L. Immunotherapeutic approaches for small-cell lung cancer. Nat Rev Clin Oncol. 2020;17(5):300-312. doi:10.1038/s41571-019-0316-z

[7] Gazdar AF, Carney DN, Nau MM, Minna JD. Characterization of variant subclasses of cell lines derived from small cell lung cancer having distinctive biochemical, morphological, and growth properties. Cancer Res. 1985;45(6):2924-2930.

[8] Gazdar AF, Carney DN, Russell EK,Sims HL, Baylin SB, Bunn PA Jr, et al. Establishment of continuous, clonable cultures of small-cell carcinoma of lung which have amine precursor uptake and decarboxylation cell properties. Cancer Res. 1980;40(10):3502-3507.

[9] Bepler G, Jaques G, Havemann K, Koehler A, Johnson BE, Gazdar AF. Characterization of two cell lines with distinct phenotypes established from a patient with small cell lung cancer. Cancer Res. 1987;47(7):1883-1891.

[10] Graziano SL, Cowan BY, Carney DN, Bryke CR, Mitter NS, Johnson BE, et al. Small cell lung cancer cell line derived from a primary tumor with a characteristic deletion of 3p. Cancer Res. 1987;47(8):2148-2155.

[11] Arvelo F, Poupon MF, Le Chevalier T. Establishment and characterization of five human small cell lung cancer cell lines from early tumor xenografts. Anticancer Res. 1994;14(5A):1893-1901.

[12] Carney DN, Gazdar AF, Bepler G, Guccion JG, Marangos PJ, Moody TW, et al. Establishment and identification of small cell lung cancer cell lines having classic and variant features. Cancer Res. 1985;45(6):2913-2923.

[13] Borromeo MD, Savage TK, Kollipara RK, He M, Augustyn A, Osborne JK, et al. ASCL1 and NEUROD1 reveal heterogeneity in pulmonary neuroendocrine tumors and regulate distinct genetic programs. Cell Rep. 2016;16(5):1259-1272. doi:10.1016/j.celrep.2016.06.081

[14] Huang YH, Klingbeil O, He XY, Wu XS, Arun G, Lu B, et al. POU2F3 is a master regulator of a tuft cell-like variant of small cell lung cancer. Genes Dev. 2018;32(13-14):915-928. doi:10.1101/gad.314815.118

[15] Baine MK, Hsieh MS, Lai WV, Egger JV, Jungbluth AA, Daneshbod Y, et al. SCLC Subtypes Defined by ASCL1, NEUROD1, POU2F3, and YAP1: A Comprehensive Immunohistochemical and Histopathologic Characterization. J Thorac Oncol. 2020;15(12):1823-1835. doi:10.1016/j.jtho.2020.09.009

[16] Gay CM, Stewart CA, Park EM, Diao L, Groves SM, Heeke S, et al. Patterns of transcription factor programs and immune pathway activation define four major subtypes of SCLC with distinct therapeutic vulnerabilities. Cancer Cell. 2021;39(3):346-360.e7. doi:10.1016/j.ccell.2020.12.014

[17] Paz-Ares L, Dvorkin M, Chen Y, Reinmuth N, Hotta K, Trukhin D, et al.

Durvalumab plus platinum-etoposide versus platinum-etoposide in first-line treatment of extensive-stage small-cell lung cancer (CASPIAN): a randomised, controlled, open-label, phase 3 trial. Lancet. 2019;394(10212):1929-1939. doi:10.1016/S0140-6736(19)32222-6

[18] Chan JM, Quintanal-Villalonga Á, Gao VR, Xie Y, Allaj V, Chaudhary O, et al. Signatures of plasticity, metastasis, and immunosuppression in an atlas of human small cell lung cancer. Cancer Cell. 2021;39(11):1479-1496.e18. doi:10.1016/j.ccell.2021.09.008

[19] Ni X, Tan Z, Ding C, Zhang C, Song L, Yang S, et al. A region-resolved mucosa proteome of the human stomach. Nat Commun. 2019;10(1):39. Published 2019 Jan 3. doi:10.1038/s41467-018-07960-x

[20] Mun DG, Bhin J, Kim S, Kim H, Jung JH, Jung Y, et al. Proteogenomic Characterization of Human Early-Onset Gastric Cancer. Cancer Cell. 2019;35(1):111-124.e10. doi:10.1016/j.ccell.2018.12.003

[21] Jiang Y, Sun A, Zhao Y, Ying W, Sun H, Yang X, et al. Proteomics identifies new therapeutic targets of early-stage hepatocellular carcinoma. Nature. 2019;567(7747):257-261. doi:10.1038/s41586-019-0987-8

[22] Gao Q, Zhu H, Dong L, Shi W, Chen R, Song Z, et al. Integrated Proteogenomic Characterization of HBV-Related Hepatocellular Carcinoma [published correction appears in Cell. 2019 Nov 14;179(5):1240]. Cell. 2019;179(2):561-577.e22. doi:10.1016/j.cell.2019.08.052

[23] Shrestha R, Llaurado Fernandez M, Dawson A, Dawson A, Hoenisch J, Volik S, et al. Multiomics Characterization of Low-Grade Serous Ovarian Carcinoma Identifies Potential Biomarkers of MEK Inhibitor Sensitivity and Therapeutic Vulnerability. Cancer Res. 2021;81(7):1681-1694. doi:10.1158/0008-5472.CAN-20-2222

[24] Li C, Sun YD, Yu GY, Cui JR, Lou Z, Zhang H, et al. Integrated Omics of Metastatic Colorectal Cancer. Cancer Cell. 2020;38(5):734-747.e9. doi:10.1016/j.ccell.2020.08.002

[25] Zhan D, Zheng N, Zhao B, Cheng F, Tang Q, Liu X, et al. Expanding individualized therapeutic options via genoproteomics. Cancer Lett. 2023;560:216123. doi:10.1016/j.canlet.2023.216123

[26] Yanagisawa K, Shyr Y, Xu BJ, Massion PP, Larsen PH, White BC. et al. Proteomic patterns of tumour subsets in non-small-cell lung cancer. Lancet. 2003;362(9382):433-439. doi:10.1016/S0140-6736(03)14068-8

[27] Xu JY, Zhang C, Wang X, Zhai L, Ma Y, Mao Y, et al. Integrative Proteomic Characterization of Human Lung Adenocarcinoma. Cell. 2020;182(1):245-261.e17. doi:10.1016/j.cell.2020.05.043

[28] Chen YJ, Roumeliotis TI, Chang YH, Chen CT, Han CL, Lin MH, et al. Proteogenomics of Non-smoking Lung Cancer in East Asia Delineates Molecular Signatures of Pathogenesis and Progression. Cell. 2020;182(1):226-244.e17. doi:10.1016/j.cell.2020.06.012

[29] Gillette MA, Satpathy S, Cao S, Dhanasekaran SM, Vasaikar SV, Krug K, et al.

Proteogenomic Characterization Reveals Therapeutic Vulnerabilities in Lung Adenocarcinoma. Cell. 2020;182(1):200-225.e35. doi:10.1016/j.cell.2020.06.013

[30] Ge S, Xia X, Ding C, Zhen B, Zhou Q, Feng J, et al. A proteomic landscape of diffuse-type gastric cancer [published correction appears in Nat Commun. 2018 May 8;9(1):1850]. Nat Commun. 2018;9(1):1012. Published 2018 Mar 8. doi:10.1038/s41467-018-03121-2

[31] Ganti AKP, Loo BW, Bassetti M, Blakely C, Chiang A, D'Amico TA, et al. Small Cell Lung Cancer, Version 2.2022, NCCN Clinical Practice Guidelines in Oncology. J Natl Compr Canc Netw. 2021;19(12):1441-1464. doi:10.6004/jnccn.2021.0058

[32] Fischbach H, Döring M, Nikles D, Lehnert E, Baldauf C, Kalinke U, et al. Ultrasensitive quantification of TAP-dependent antigen compartmentalization in scarce primary immune cell subsets. Nat Commun. 2015;6:6199. Published 2015 Feb 6. doi:10.1038/ncomms7199

[33] Palomar G, Dudek K, Wielstra B, Jockusch EL, Vinkler M, Arntzen JW, et al. Molecular Evolution of Antigen-Processing Genes in Salamanders: Do They Coevolve with MHC Class I Genes? [published correction appears in Genome Biol Evol. 2021 Apr 5;13(4):]. Genome Biol Evol. 2021;13(2):evaa259. doi:10.1093/gbe/evaa259

[34] Leverson JD, Sampath D, Souers AJ, Rosenberg SH, Fairbrother WJ, Amiot M, et al. Found in Translation: How Preclinical Research Is Guiding the Clinical Development of the BCL2-Selective Inhibitor Venetoclax. Cancer Discov. 2017;7(12):1376-1393. doi:10.1158/2159-8290.CD-17-0797

[35] Hata AN, Engelman JA, Faber AC. The BCL2 Family: Key Mediators of the Apoptotic Response to Targeted Anticancer Therapeutics. Cancer Discov. 2015;5(5):475-487. doi:10.1158/2159-8290.CD-15-0011

[36] Duan R, Du W, Guo W. EZH2: a novel target for cancer treatment. J Hematol Oncol. 2020;13(1):104. Published 2020 Jul 28. doi:10.1186/s13045-020-00937-8

[37] Petersen SL, Chen TT, Lawrence DA, Marsters SA, Gonzalvez F, Ashkenazi A. TRAF2 is a biologically important necroptosis suppressor. Cell Death Differ. 2015;22(11):1846-1857. doi:10.1038/cdd.2015.35

[38] Cheng Y, Han L, Wu L, Chen J, Sun H, Wen G, et al. Effect of First-Line Serplulimab vs Placebo Added to Chemotherapy on Survival in Patients With Extensive-Stage Small Cell Lung Cancer: The ASTRUM-005 Randomized Clinical Trial. JAMA. 2022;328(12):1223-1232.

[39] El Sayed R, Blais N. Immunotherapy in Extensive-Stage Small Cell Lung Cancer. Curr Oncol. 2021;28(5):4093-4108. Published 2021 Oct 12. doi:10.3390/curroncol28050347

[40] Gardner EE, Lok BH, Schneeberger VE, Desmeules P, Miles LA, Arnold PK, et al. Chemosensitive Relapse in Small Cell Lung Cancer Proceeds through an EZH2-SLFN11 Axis. Cancer Cell. 2017;31(2):286-299.

[41] No authors listed. First EZH2 Inhibitor Approved-for Rare Sarcoma. Cancer Discov. 2020;10(3):333-334.

[42] Zhou L, Mudianto T, Ma X, Riley R, Uppaluri R. Targeting EZH2 Enhances Antigen Presentation, Antitumor Immunity, and Circumvents Anti-PD-1 Resistance

in Head and Neck Cancer. Clin Cancer Res. 2020;26(1):290-300.

[43] Moore AM, Einhorn LH, Estes D, Govindan R, Axelson J, Vinson J, et al. Gefitinib in patients with chemo-sensitive and chemo-refractory relapsed small cell cancers: a Hoosier Oncology Group phase II trial. Lung Cancer. 2006;52(1):93-97.

[44] Arnold D, Lueza B, Douillard JY, Peeters M, Lenz HJ, Venook A, et al. Prognostic and predictive value of primary tumour side in patients with RAS wild-type metastatic colorectal cancer treated with chemotherapy and EGFR directed antibodies in six randomized trials. Ann Oncol. 2017;28(8):1713-1729. doi:10.1093/annonc/mdx175

[45] Mak DWS, Li S, Minchom A. Challenging the recalcitrant disease-developing molecularly driven treatments for small cell lung cancer. Eur J Cancer. 2019;119:132-150.

[46] Held L, Siu C, Shadman M. Venetoclax as a therapeutic option for the treatment of chronic lymphocytic leukemia: the evidence so far. Expert Opin Pharmacother. 2021;22(6):655-665.

[47] Lochmann TL, Floros KV, Naseri M, Powell KM, Cook W, March RJ, et al. Venetoclax Is Effective in Small-Cell Lung Cancers with High BCL-2 Expression. Clin Cancer Res. 2018;24(2):360-369.

[48] Liewer S, Huddleston A. Alisertib: a review of pharmacokinetics, efficacy and toxicity in patients with hematologic malignancies and solid tumors. Expert Opin Investig Drugs. 2018;27(1):105-112.

[49] Vénéreau E, Ceriotti C, Bianchi ME. DAMPs from Cell Death to New Life. Front Immunol. 2015;6:422. Published 2015 Aug 18.

[50] Sprooten J, De Wijngaert P, Vanmeerbeerk I, Martin S, Vangheluwe P, Schlenner S, et al. Necroptosis in Immuno-Oncology and Cancer Immunotherapy. Cells. 2020;9(8):1823.

[51] Bist P, Leow SC, Phua QH, Shu S, Zhuang Q, Loh WT, et al. Annexin-1 interacts with NEMO and RIP1 to constitutively activate IKK complex and NF-κB: implication in breast cancer metastasis. Oncogene. 2011;30(28):3174-3185.

[52] Park S, Hatanpaa KJ, Xie Y, Mickey BE, Madden CJ, Raisanen JM, et al. The receptor interacting protein 1 inhibits p53 induction through NF-kappaB activation and confers a worse prognosis in glioblastoma. Cancer Res. 2009;69(7):2809-2816.

[53] McCormick KD, Ghosh A, Trivedi S, Wang L, Coyne CB, Ferris RL, et al. Innate immune signaling through differential RIPK1 expression promote tumor progression in head and neck squamous cell carcinoma. Carcinogenesis. 2016;37(5):522-529.

[54] Li X, Guo J, Ding AP, Qi WW, Zhang PH, Lv J, et al. Association of Mixed Lineage Kinase Domain-Like Protein Expression With Prognosis in Patients With Colon Cancer. Technol Cancer Res Treat. 2017;16(4):428-434.

[55] Li L, Yu S, Zang C. Low Necroptosis Process Predicts Poor Treatment Outcome of Human Papillomavirus Positive Cervical Cancers by Decreasing Tumor-Associated Macrophages M1 Polarization. Gynecol Obstet Invest. 2018;83(3):259-267.

[56] He L, Peng K, Liu Y, Xiong J, Zhu FF. Low expression of mixed lineage kinase

domain-like protein is associated with poor prognosis in ovarian cancer patients. Onco Targets Ther. 2013;6:1539-1543.

[57] Colbert LE, Fisher SB, Hardy CW, Hall WA, Saka B, Shelton JW, et al. Pronecrotic mixed lineage kinase domain-like protein expression is a prognostic biomarker in patients with early-stage resected pancreatic adenocarcinoma. Cancer. 2013;119(17):3148-3155.

[58] Jiao D, Cai Z, Choksi S, Ma D, Choe M, Kwon HJ, et al. Necroptosis of tumor cells leads to tumor necrosis and promotes tumor metastasis. Cell Res. 2018;28(8):868-870.

[59] Ruan J, Mei L, Zhu Q, Shi G, Wang H. Mixed lineage kinase domain-like protein is a prognostic biomarker for cervical squamous cell cancer. Int J Clin Exp Pathol. 2015;8(11):15035-15038.

[60] Ertao Z, Jianhui C, Kang W, hijun Y, Hui W, Chuangqi C, et al. Prognostic value of mixed lineage kinase domain-like protein expression in the survival of patients with gastric caner. Tumour Biol. 2016;37(10):13679-13685.

[61] Yang C, Sengupta S, Hegde PM, Mitra J, Jiang S, Holey B, et al. Regulation of oxidized base damage repair by chromatin assembly factor 1 subunit A. Nucleic Acids Res. 2017;45(2):739-748.

[62] Nera B, Huang HS, Lai T, Xu L. Elevated levels of TRF2 induce telomeric ultrafine anaphase bridges and rapid telomere deletions. Nat Commun. 2015;6:10132.

[63] Lee JH, You J, Dobrota E, Skalnik DG. Identification and characterization of a novel human PP1 phosphatase complex. J Biol Chem. 2010;285(32):24466-24476.

[64] Nayak A, Dutta M, Roychowdhury A. Emerging oncogene ATAD2: Signaling cascades and therapeutic initiatives. Life Sci. 2021;276:119322.

[65] Burrell RA, McClelland SE, Endesfelder D, Groth P, Weller MC, Shaikh N, et al. Replication stress links structural and numerical cancer chromosomal instability [published correction appears in Nature. 2013 Aug 22;500(7463):490]. Nature. 2013;494(7438):492-496.

[66] Feng W, Yonezawa M, Ye J, Jenuwein T, Grummt I. PHF8 activates transcription of rRNA genes through H3K4me3 binding and H3K9me1/2 demethylation. Nat Struct Mol Biol. 2010;17(4):445-450.

[67] Lee YC, Kim YJ. Requirement for a functional interaction between mediator components Med6 and Srb4 in RNA polymerase II transcription. Mol Cell Biol. 1998;18(9):5364-5370.

[68] Feng J, Ding C, Qiu N, Ni X, Zhan D, Liu W, et al. Firmiana: towards a one-stop proteomic cloud platform for data processing and analysis. Nat Biotechnol. 2017;35(5):409-412. doi:10.1038/nbt.3825

[69] Huang W, Zhan D, Li Y, Zheng N, Wei X, Bai B, et al. Proteomics provides individualized options of precision medicine for patients with gastric cancer. ***Sci China Life Sci.*** 2021 Aug;64(8):1199-1211. doi: 10.1007/s11427-021-1966-4. Epub

2021 Jul 9. PMID: 34258712.

Figure legends

Figure 1 Study design and key clinical characteristics of the SCLC patients from the discovery cohort

A. A flowchart of our study scheme. **B.** clinical characteristics of the patients from the discovery cohort. **C.**The Kaplan-Meier plot shows the limited predictive value on patient overall survival of the VALG, TNM, and ASCL1/NeuroD1 staging and classification methods. VALG, Veterans Administration Lung Study Group;

Figure 2. Proteomics stratifies SCLC into subtypes that correlate with clinical outcomes. A. In the discovery cohort, NMF clustering yielded three subgroups in SCLC. **B.** The three subtypes based on proteomic profiling were associated with different clinical outcomes. **C.** In the validation cohort, biopsy samples were obtained from the First Affiliated Hospital of Henan University. The predictive classifier model shows the prognosis trend similar to the discovery cohort. **D.** The three proteomic subtypes exhibited different responses to chemotherapy. S-I, Log-rank *P*-value = 0.023. S-II, Log-rank *P*-value = 0.042. S-III, Log-rank *P*-value = 0.15.

Figure 3. Differential signature proteins and enriched biological processes in proteomic SCLC subtypes. A. Heatmap of signature proteins in each subtype. **B.** Metascape functional enrichment analysis identified different biological processes or pathways activated in the three subtypes. **C-D.** the MHC-I(**C**) rather than MHC-II (**D**) molecules were highly expressed in S-II compared with S-I and S-III.

Figure 4. A. the clinical characteristics of the patients from the immunotherapy cohort. **B-C.** In the immunotherapy cohort, the S-II patients had the best PFS time when receiving first-line immunotherapy (**B**) but showed no statistically obvious difference between S-I/III when receiving second-line immunotherapy (**C**). **D.** In all S-II patients, patients had better overall survival after immunotherapy compared with those did not received immunotherapy.

Figure 5. The atlas of potential drug targets for individual patients in S-III.

Supplementary material

Figure S1 Univariate prognostic analysis of common clinical pathological factors

Figure S2. Representative IHC staining and distribution of common neuroendocrine biomarkers in SCLC. **A.** Representative IHC staining of ASCL1, NeuroD1, and YAP1. **B.** The expression of ASCL1, NeuroD1, and YAP1 was not distributed differently across the three subtypes.

Figure S3. SCLC proteomic subtype was an independent prognostic factor confirmed by multivariate Cox analysis.

Table S1. Clinical- pathological data of discovery cohort.
Table S2. Proteomic results(FOT) of each case in the discovery cohort.
Table S3. Proteins for the non-negative matrix factorization (NMF) consensus clustering.
Table S4. Fifty-eight signature proteins for the predictive classifier model.
Table S5. Clinical- pathological data of validation cohort.
Table S6. Proteomic results(FOT) of each case in the validation cohort.
Table S7. Signature proteins for each subtype.
Table S8. Clinical- pathological data of the immunotherapy cohort.
Table S9. Proteomic results(FOT) of each case in the immunotherapy cohort.

Figure 1

A

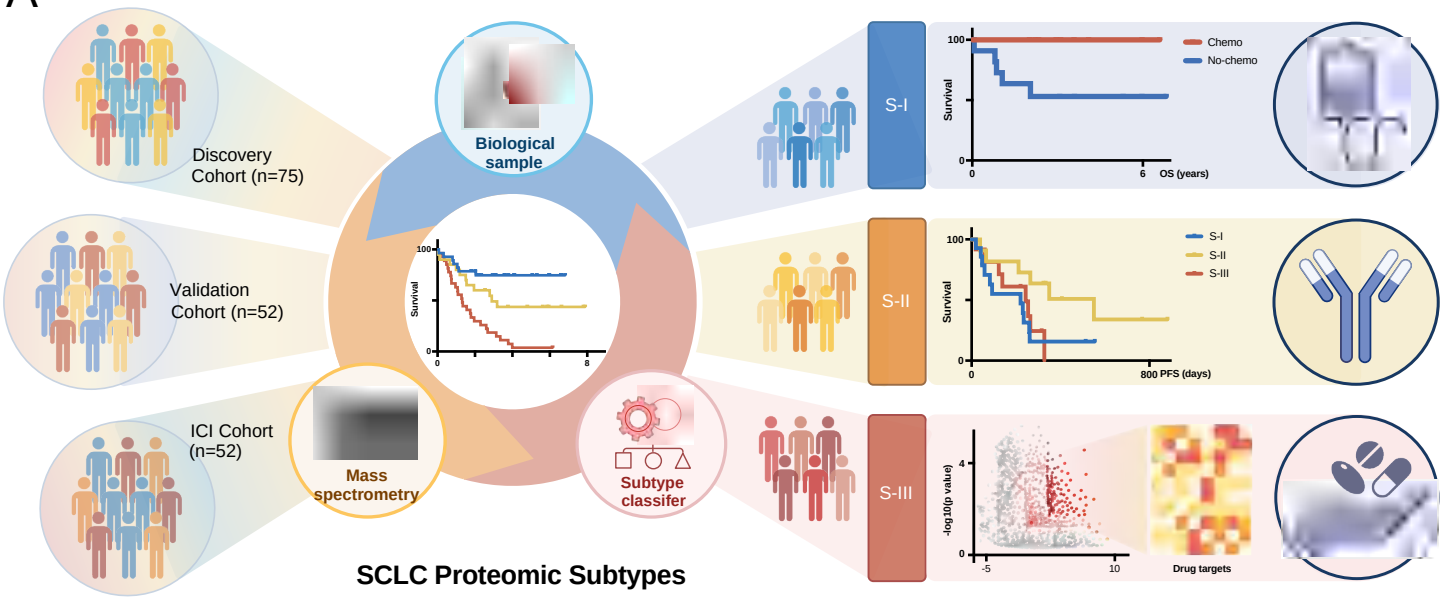
Discovery Cohort (n=75)
Validation Cohort (n=52)
ICI Cohort (n=52)
Biological sample
Mass spectrometry
Subtype classifer
SCLC Proteomic Subtypes
S-I
S-II
S-III
Survival
Chemo
No-chemo
OS (years)
800 PFS (days)
-log10(p value)
Drug targets

B

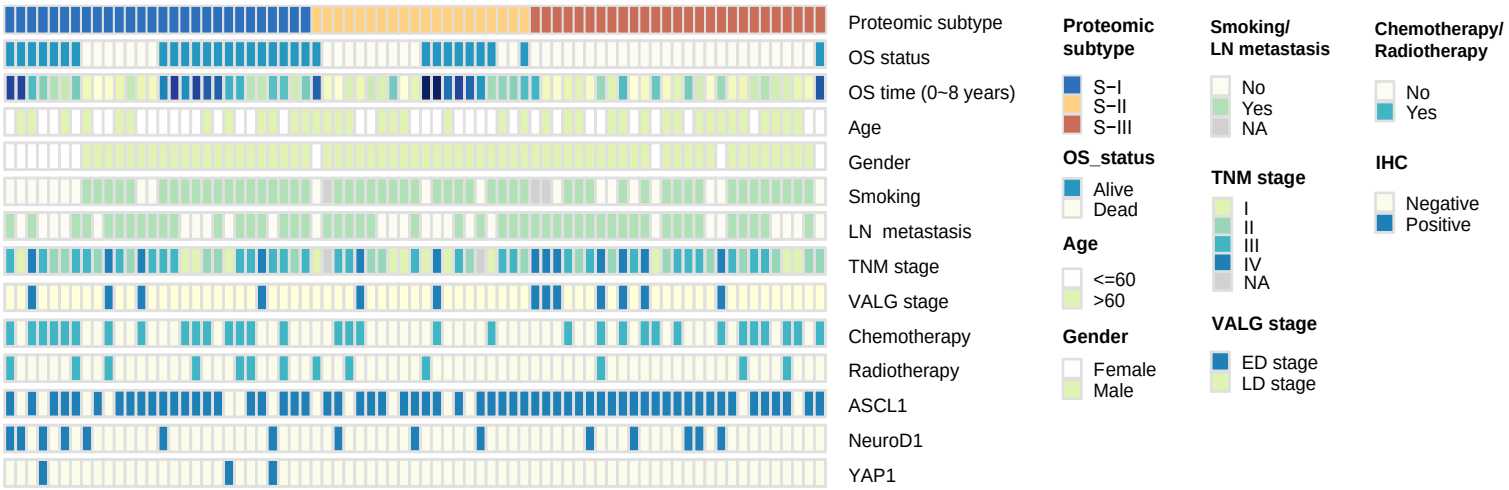
Proteomic subtype
OS status
OS time (0~8 years)
Age
Gender
Smoking
LN metastasis
TNM stage
VALG stage
Chemotherapy
Radiotherapy
ASCL1
NeuroD1
YAP1
Proteomic subtype
S−I
S−II
S−III
OS_status
Alive
Dead
Age
<=60
>60
Gender
Female
Male
Smoking/ LN metastasis
No
Yes
NA
TNM stage
I
II
III
IV
NA
VALG stage
ED stage
LD stage
Chemotherapy/ Radiotherapy
No
Yes
IHC
Negative
Positive

C

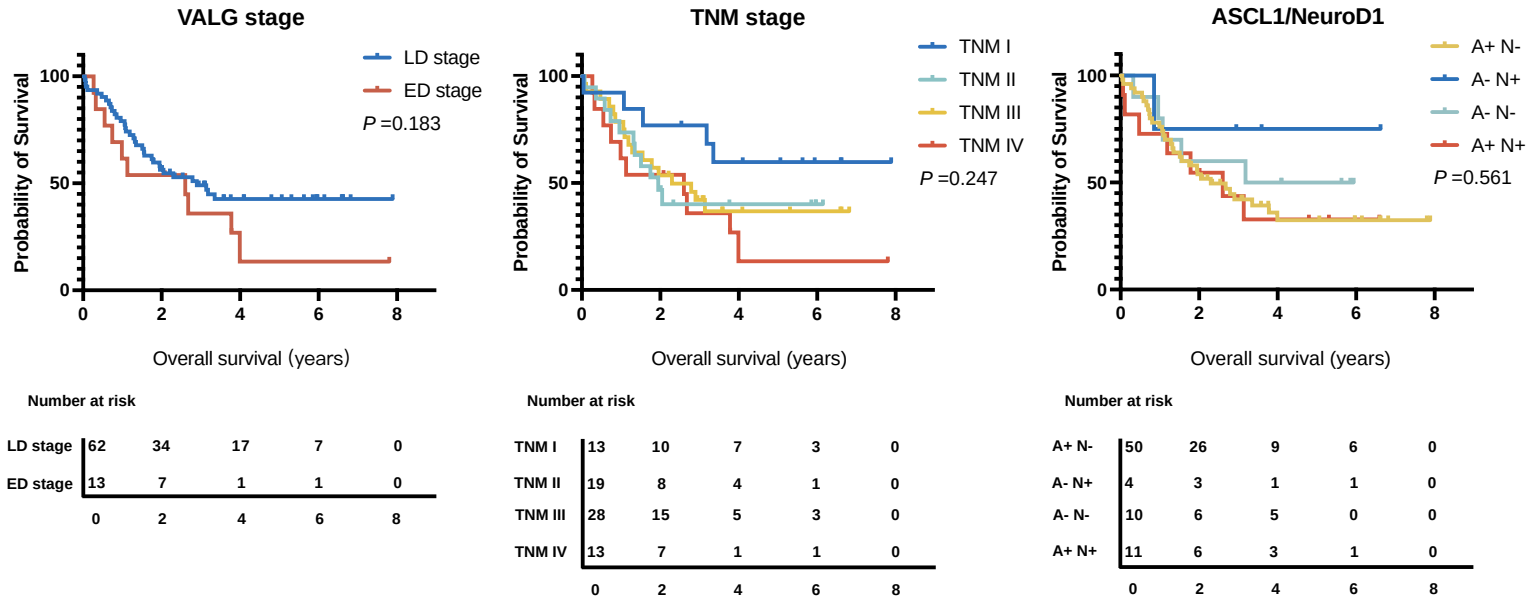
VALG stage
LD stage
ED stage
P =0.183
Probability of Survival
Overall survival (years)
Number at risk
LD stage 62 34 17 7 0
ED stage 13 7 1 1 0
0 2 4 6 8
TNM stage
TNM I
TNM II
TNM III
TNM IV
P =0.247
Probability of Survival
Overall survival (years)
Number at risk
TNM I 13 10 7 3 0
TNM II 19 8 4 1 0
TNM III 28 15 5 3 0
TNM IV 13 7 1 1 0
0 2 4 6 8
ASCL1/NeuroD1
A+ N-
A- N+
A- N-
A+ N+
P =0.561
Probability of Survival
Overall survival (years)
Number at risk
A+ N- 50 26 9 6 0
A- N+ 4 3 1 1 0
A- N- 10 6 5 0 0
A+ N+ 11 6 3 1 0
0 2 4 6 8

Figure 2

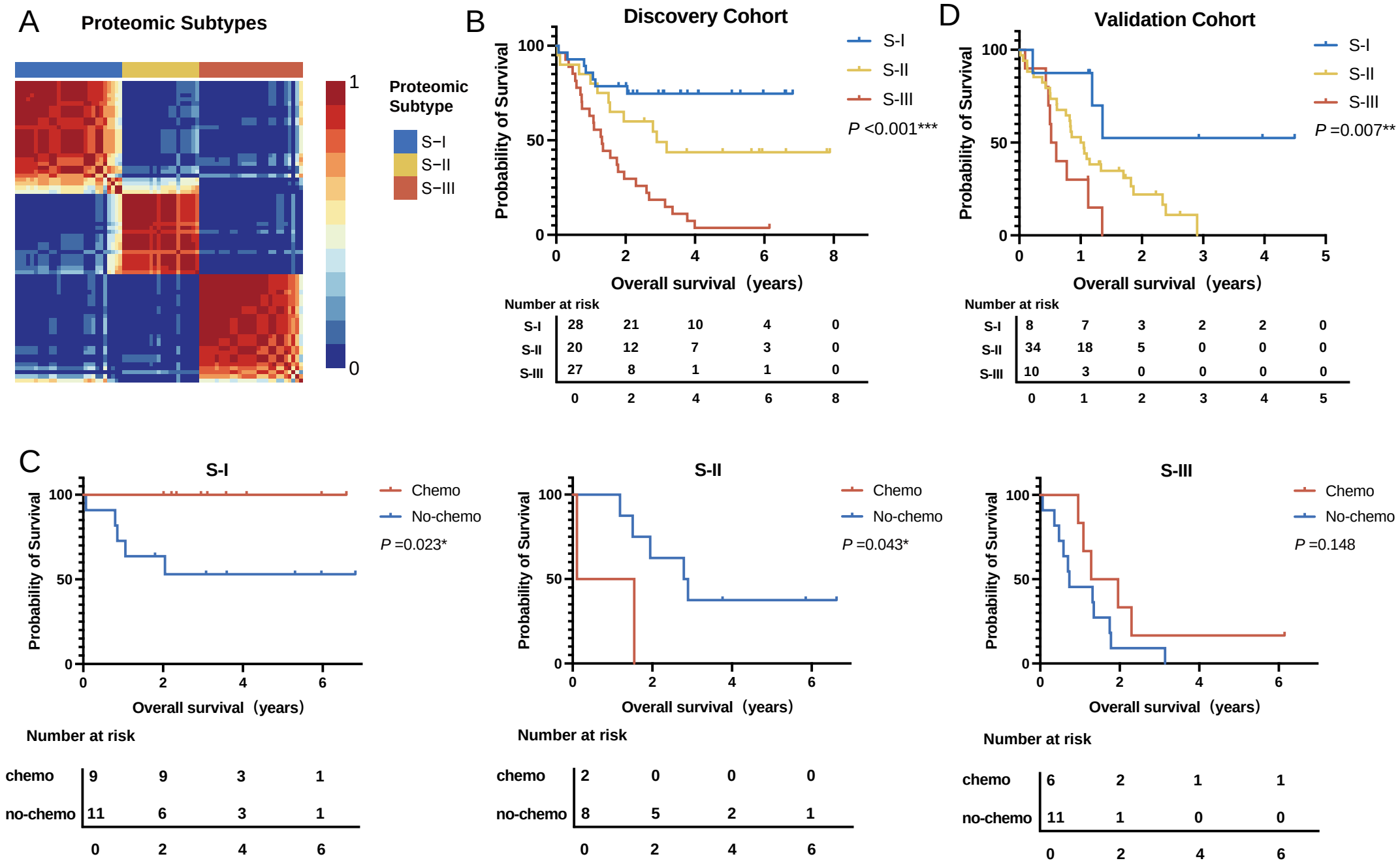
A
Proteomic Subtypes
1
0
Proteomic Subtype
S−I
S−II
S−III
B
Discovery Cohort
Probability of Survival
100
50
0
0
2
4
6
8
Overall survival（years）
S-I
S-II
S-III
P <0.001***
Number at risk
S-I 28 21 10 4 0
S-II 20 12 7 3 0
S-III 27 8 1 1 0
0 2 4 6 8
D
Validation Cohort
Probability of Survival
100
50
0
0
1
2
3
4
5
Overall survival（years）
S-I
S-II
S-III
P =0.007**
Number at risk
S-I 8 7 3 2 2 0
S-II 34 18 5 0 0 0
S-III 10 3 0 0 0 0
0 1 2 3 4 5
C
S-I
Probability of Survival
100
50
0
0
2
4
6
Overall survival（years）
Chemo
No-chemo
P =0.023*
Number at risk
chemo 9 9 3 1
no-chemo 11 6 3 1
0 2 4 6
S-II
Probability of Survival
100
50
0
0
2
4
6
Overall survival（years）
Chemo
No-chemo
P =0.043*
Number at risk
chemo 2 0 0 0
no-chemo 8 5 2 1
0 2 4 6
S-III
Probability of Survival
100
50
0
0
2
4
6
Overall survival（years）
Chemo
No-chemo
P =0.148
Number at risk
chemo 6 2 1 1
no-chemo 11 1 0 0
0 2 4 6

Figure 3

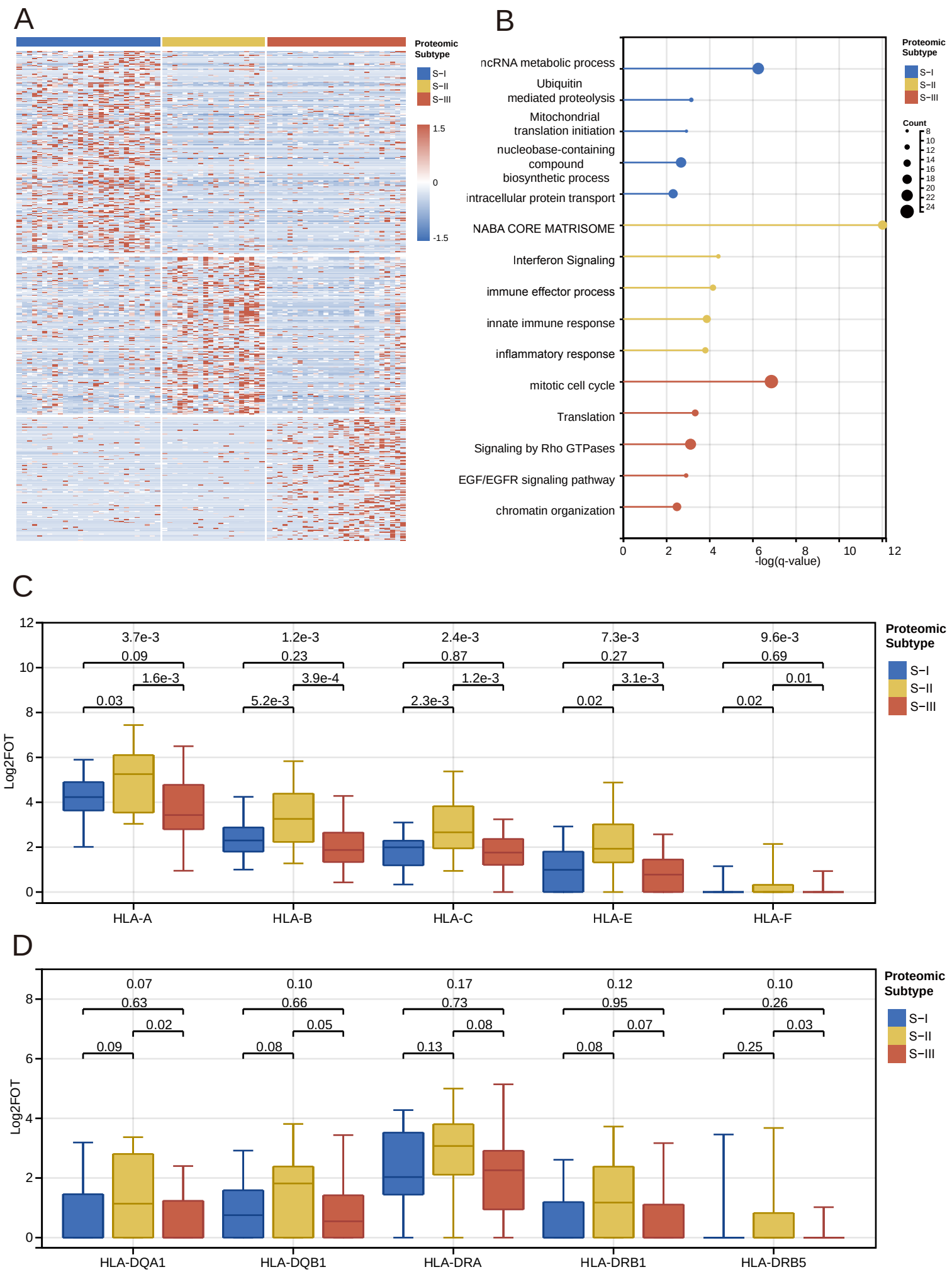
A
Proteomic Subtype
S−I
S−II
S−III
1.5
0
-1.5
B
ncRNA metabolic process
Ubiquitin mediated proteolysis
Mitochondrial translation initiation
nucleobase-containing compound biosynthetic process
intracellular protein transport
NABA CORE MATRISOME
Interferon Signaling
immune effector process
innate immune response
inflammatory response
mitotic cell cycle
Translation
Signaling by Rho GTPases
EGF/EGFR signaling pathway
chromatin organization
0 2 4 6 8 10 12
-log(q-value)
Count
8 10 12 14 16 18 20 22 24
C
Log2FOT
3.7e-3 0.09 1.6e-3 0.03
1.2e-3 0.23 3.9e-4 5.2e-3
2.4e-3 0.87 1.2e-3 2.3e-3
7.3e-3 0.27 3.1e-3 0.02
9.6e-3 0.69 0.01 0.02
HLA-A
HLA-B
HLA-C
HLA-E
HLA-F
D
Log2FOT
0.07 0.63 0.02 0.09
0.10 0.66 0.05 0.08
0.17 0.73 0.08 0.13
0.12 0.95 0.07 0.08
0.10 0.26 0.03 0.25
HLA-DQA1
HLA-DQB1
HLA-DRA
HLA-DRB1
HLA-DRB5

Figure 4

A

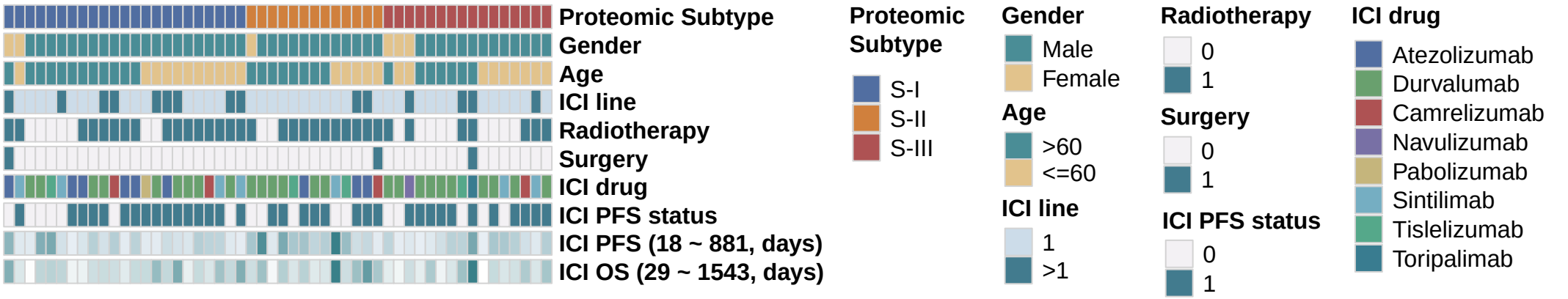

B

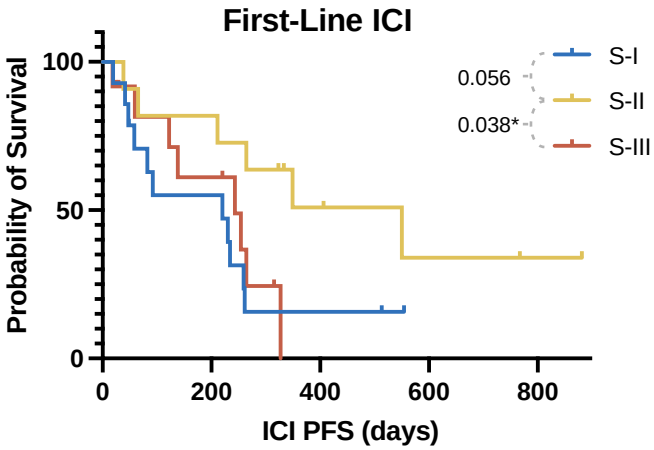

Number at risk

S-I	14	7	2	0	0
S-II	11	9	4	2	1
S-III	12	6	0	0	0
	0	200	400	600	800

C

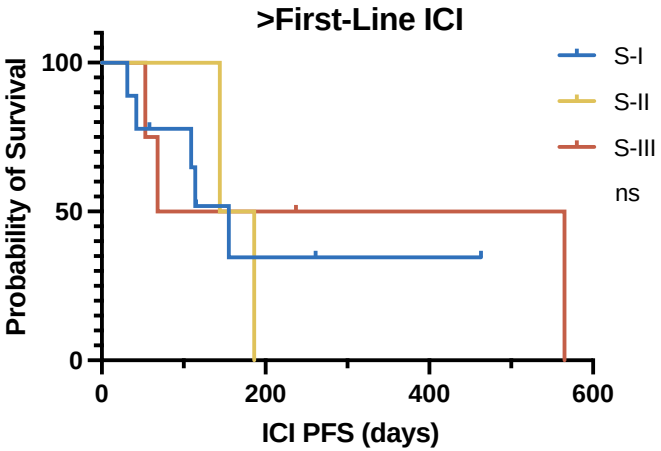

Number at risk

S-I	9	2	1	0
S-II	2	0	0	0
S-III	4	2	1	0
	0	200	400	600

D

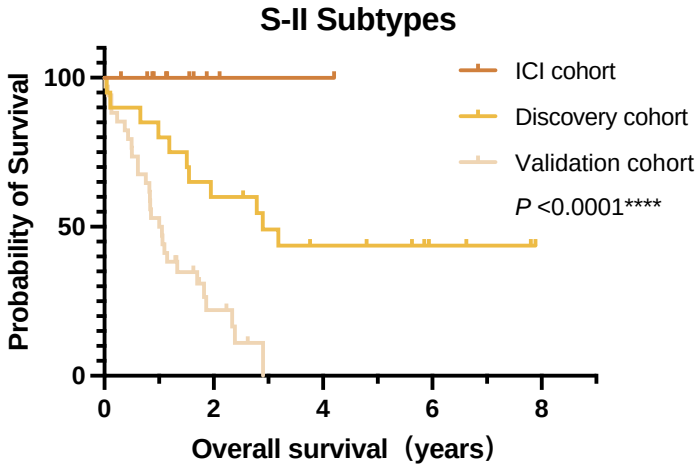

Number at risk

ICI cohort	13	4	1	1	1
Discovery cohort	20	12	7	4	1
Validation cohort	34	5	1	1	1
	0	2	4	6	8

Figure 5

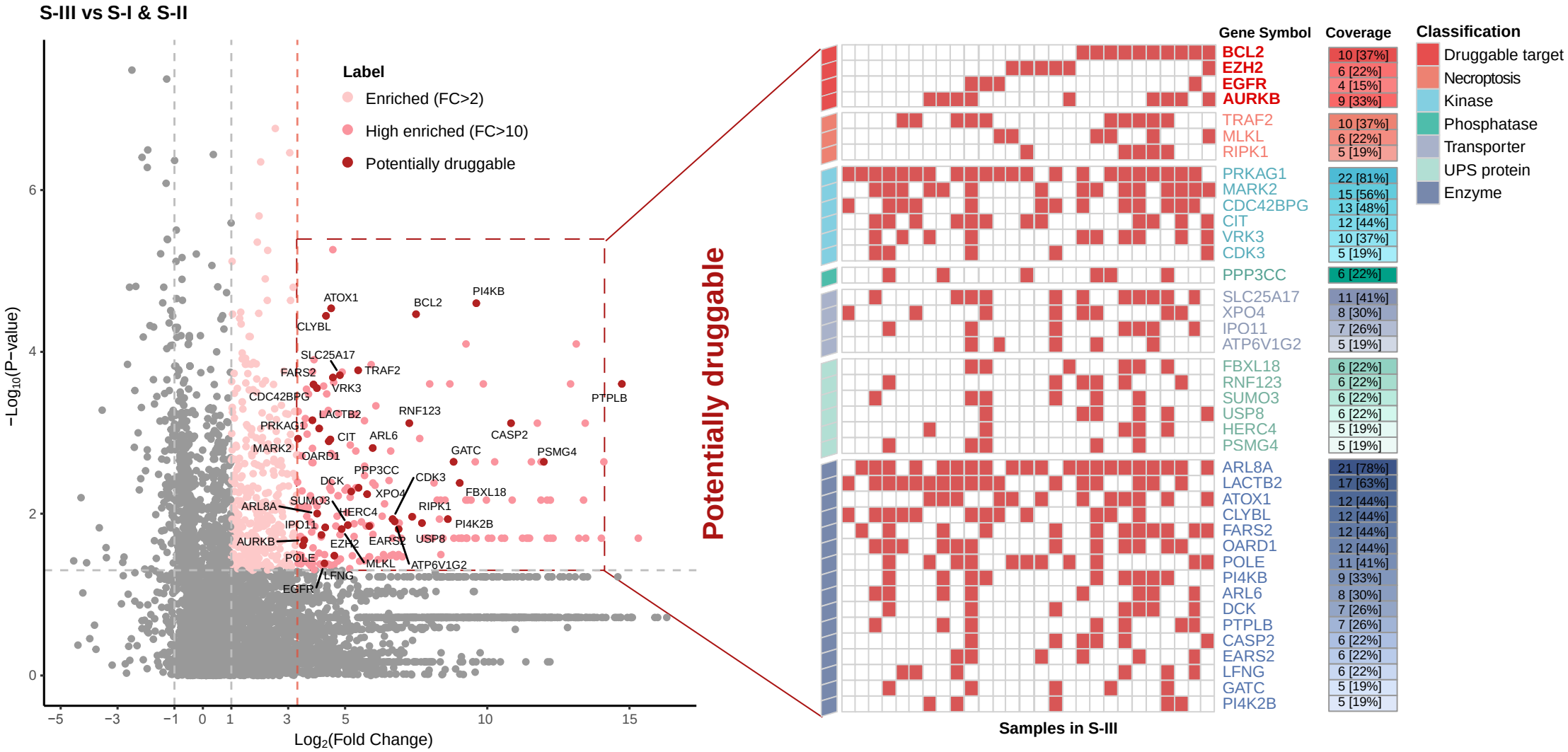
S-III vs S-I & S-II
Label
Enriched (FC>2)
High enriched (FC>10)
Potentially druggable
−Log10(P−value)
Log2(Fold Change)
ATOX1
BCL2
PI4KB
CLYBL
SLC25A17
FARS2
TRAF2
VRK3
CDC42BPG
PTPLB
LACTB2
RNF123
PRKAG1
CIT
ARL6
CASP2
MARK2
OARD1
GATC
PSMG4
PPP3CC
DCK
CDK3
XPO4
FBXL18
SUMO3
ARL8A
HERC4
RIPK1
IPO11
PI4K2B
AURKB
EZH2
EARS2
USP8
POLE
MLKL
ATP6V1G2
LFNG
EGFR
Potentially druggable
Gene Symbol
Coverage
Classification
BCL2 10 [37%]
EZH2 6 [22%]
EGFR 4 [15%]
AURKB 9 [33%]
TRAF2 10 [37%]
MLKL 6 [22%]
RIPK1 5 [19%]
PRKAG1 22 [81%]
MARK2 15 [56%]
CDC42BPG 13 [48%]
CIT 12 [44%]
VRK3 10 [37%]
CDK3 5 [19%]
PPP3CC 6 [22%]
SLC25A17 11 [41%]
XPO4 8 [30%]
IPO11 7 [26%]
ATP6V1G2 5 [19%]
FBXL18 6 [22%]
RNF123 6 [22%]
SUMO3 6 [22%]
USP8 6 [22%]
HERC4 5 [19%]
PSMG4 5 [19%]
ARL8A 21 [78%]
LACTB2 17 [63%]
ATOX1 12 [44%]
CLYBL 12 [44%]
FARS2 12 [44%]
OARD1 12 [44%]
POLE 11 [41%]
PI4KB 9 [33%]
ARL6 8 [30%]
DCK 7 [26%]
PTPLB 7 [26%]
CASP2 6 [22%]
EARS2 6 [22%]
LFNG 6 [22%]
GATC 5 [19%]
PI4K2B 5 [19%]
Samples in S-III
Druggable target
Necroptosis
Kinase
Phosphatase
Transporter
UPS protein
Enzyme

Supplement figure 1

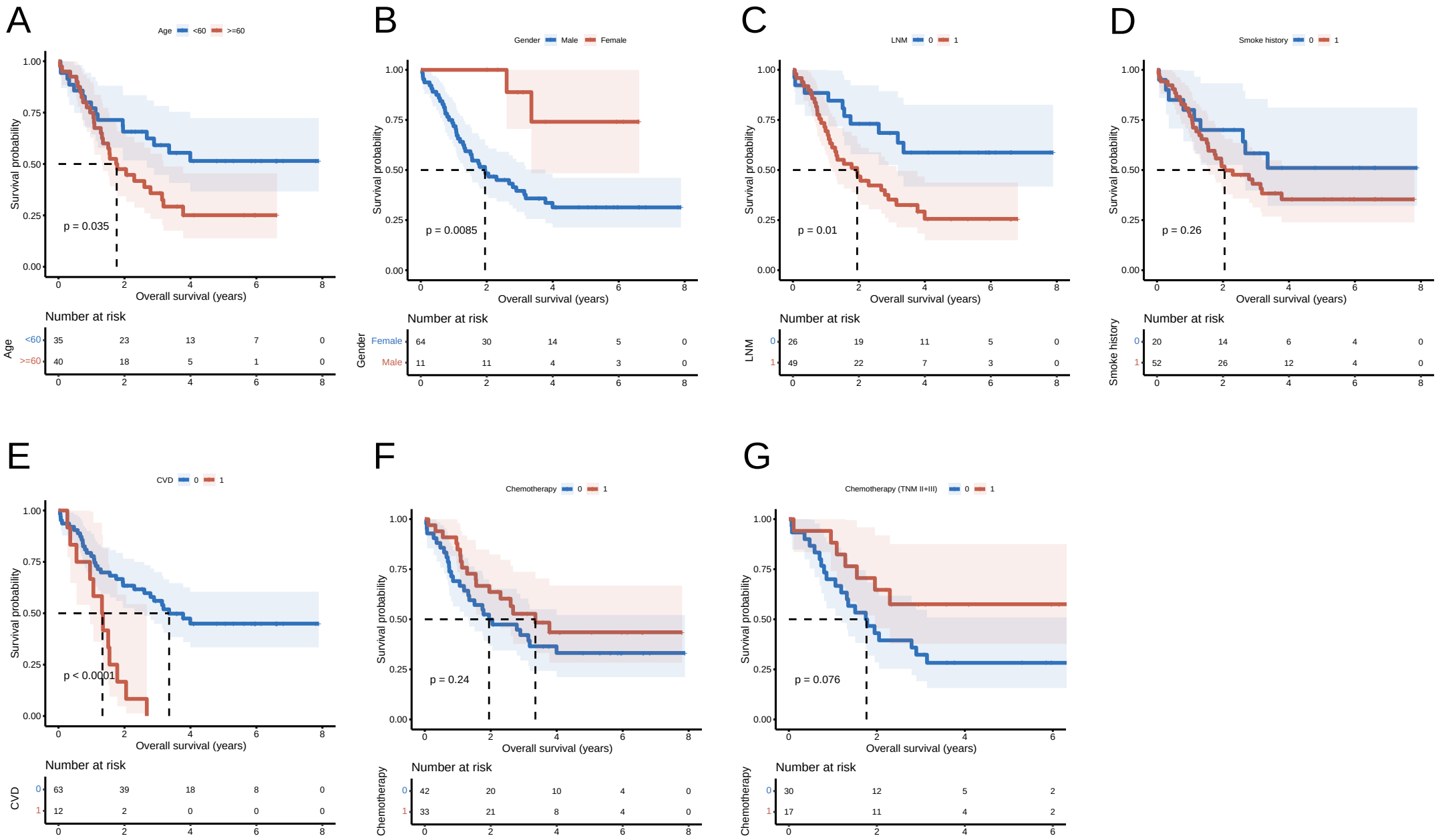

Supplement figure 2

A

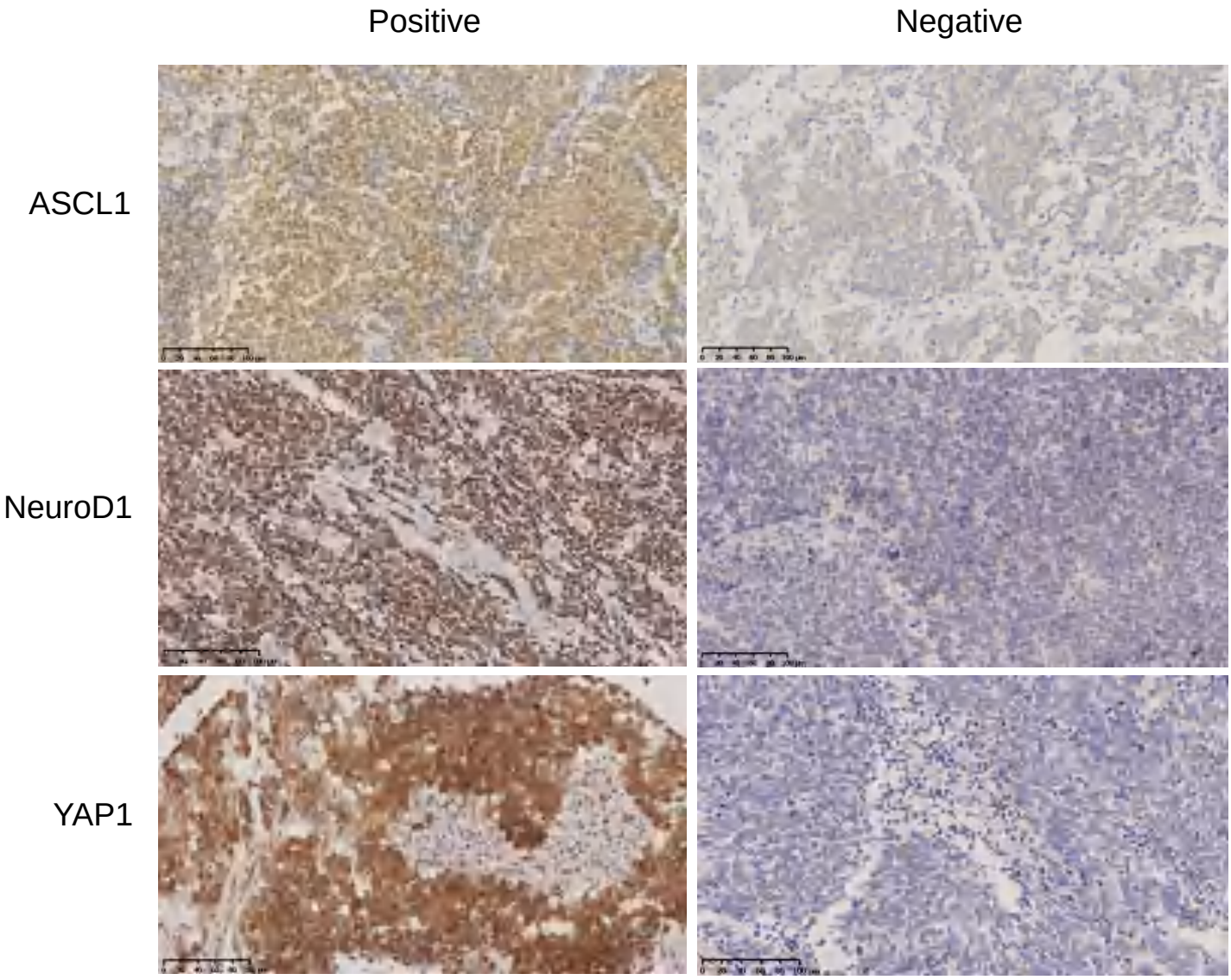

B

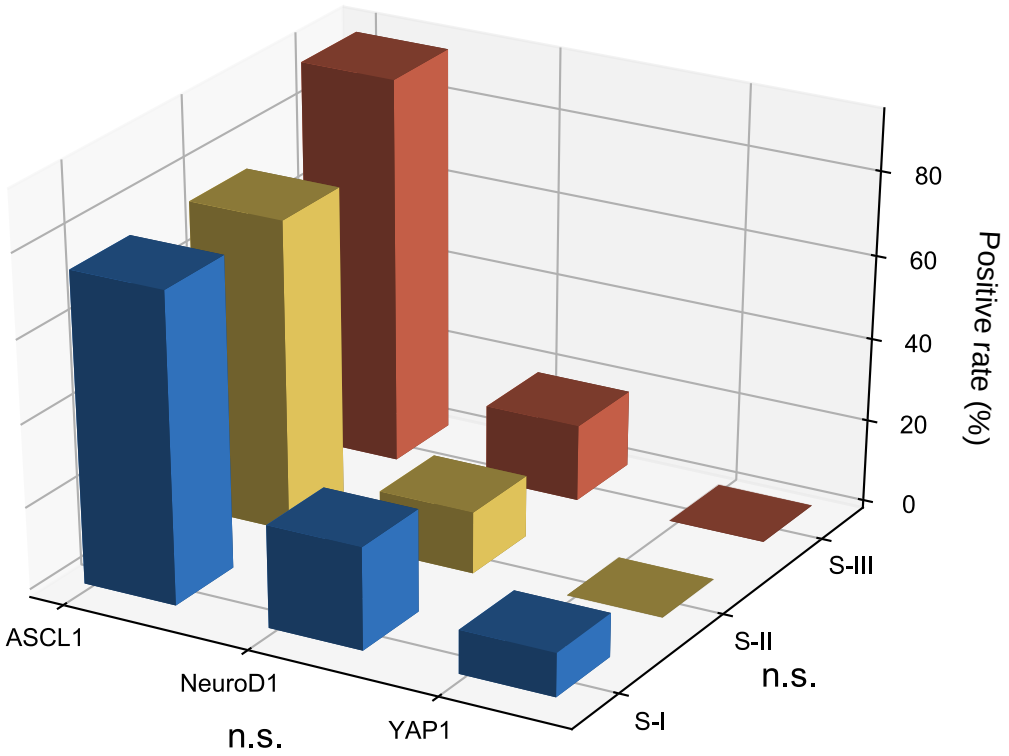

Supplement figure 3
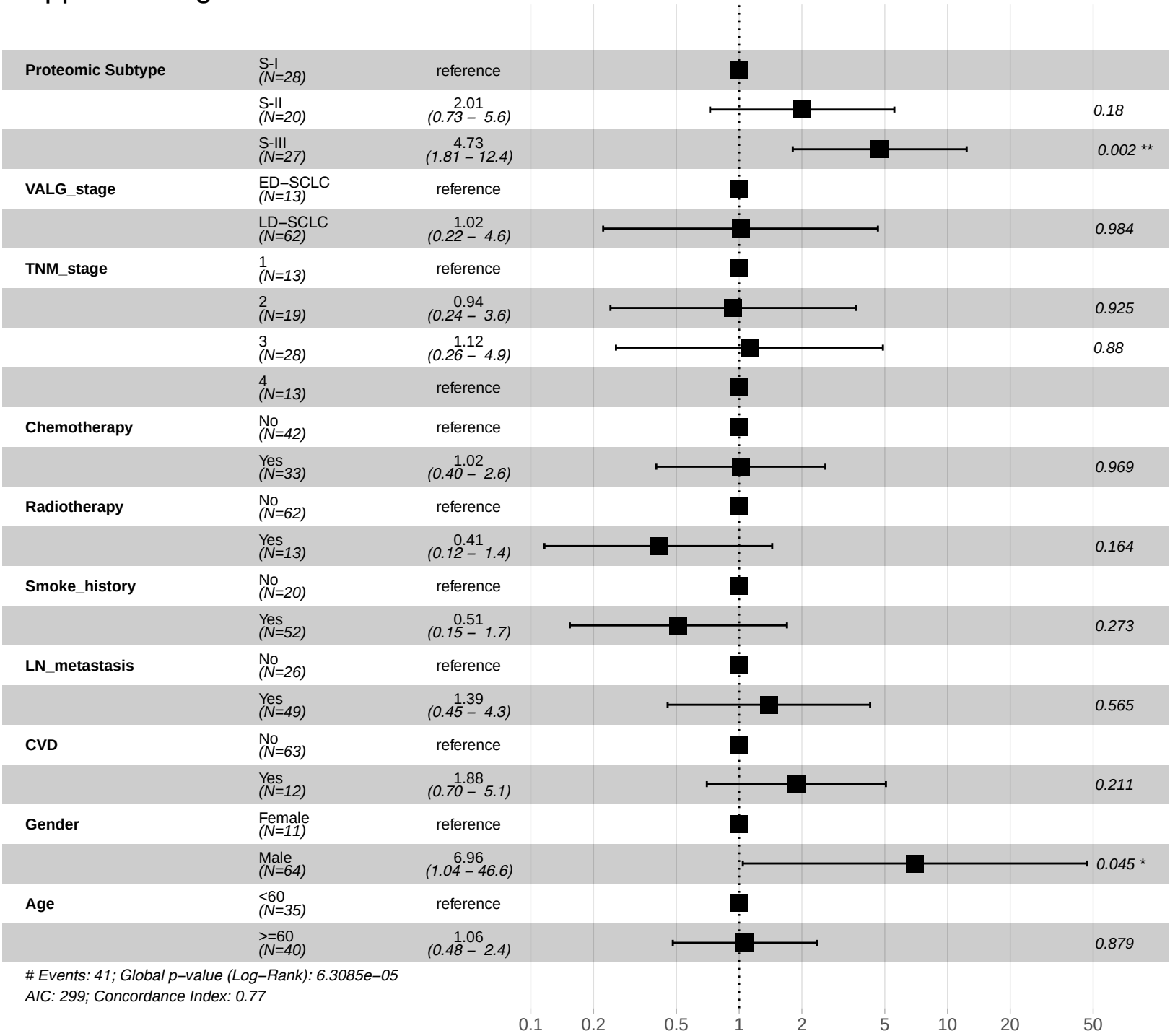
Multivariate Cox analysis